

Ligand Bridged Heterodinuclear Transition Metal Complexes – Syntheses, Structures and Electrochemical Investigations

Petra Escarpa Gaede* and Christoph van Wüllen

Berlin, Technische Universität, Institut für Chemie

Received May 5th, 2005.

Dedicated to Professor Jörn Müller on the Occasion of his 70th Birthday

Abstract. The syntheses of the homo- and heterobimetallic compounds $[L_n^1M(\eta^5-C_5H_4)CMe_2(\eta^5-C_9H_6)^2ML_n]$ (**2a–5d**), $[(C_9H_7)CMe_2(\eta^5-C_5H_4)Fe(\eta^5-C_5H_4)CMe_2(\eta^5-C_9H_6)^2ML_n]$ (**6a–c**), and $[(\eta^5-C_5H_4)CMe_2(\eta^5-C_9H_6)^2ML_n]_2Fe$ (**7a–b**) are reported with $^1ML_n = Rh(cod)$ **2**, $Ir(cod)$ **3**, $Mn(CO)_3$ **4** and $FeCp$ **5**, $^2ML_n = Rh(cod)$ **a**, $Ir(cod)$ **b**, $Mn(CO)_3$ **c** and $FeCp$ **d**, respectively. Crystal structures of **3a**, **3b** and **5c** are described showing two different ligand conformations in form of two rotamers. The energetic difference between these both rotamers is insignificant small in the gas phase according to DFT calculations. The rotation barrier for the species has been determined to 23 kJ/mol. According to the absence of intermolecular interactions in the solid state, the preference for one of the conformers is deduced from packing effects.

All complexes are investigated by cyclic voltammetry. The shift of the redox potentials with respect to the mononuclear reference systems is a suitable tool to determine intermetallic electronic interaction. For some compounds, the normal behaviour with an increasing separation of the redox potentials is observed. A second group of complexes shows the opposite behaviour with a decreasing in the potential differences. A mechanism of intramolecular catalytic oxidation is supposed for that species.

Keywords: Organometallic compounds; Heterobimetallic compounds; Metal-metal interactions; Cyclic voltammetry, Conformation analysis

Introduction

Bimetallic complexes have found much interest in the last decade. Cooperative effects involving two metal centers kept in close proximity by a bridging ligand have led to unprecedented reactivity in stoichiometric or catalytic reactions [1]. Extensive work has been concentrated on Cp systems linked by methylene or dimethylsilylene units [2] because the strong metal-Cp bond prevents the dissociation into two mononuclear metal complex fragments during the reaction [3]. Furthermore, various metal atoms in different oxidation states can be bounded to such ligands. This has led to a number of binuclear complexes of type A (see fig. 1), which can be further classified as homo- or heterobimetallic species. While the synthesis of homonuclear compounds presents no particular difficulty for this ligand system, its symmetrical structure makes the selective preparation of bimetallic complexes problematic. The reason is that the deprotonation/metallation reaction used to introduce a metal

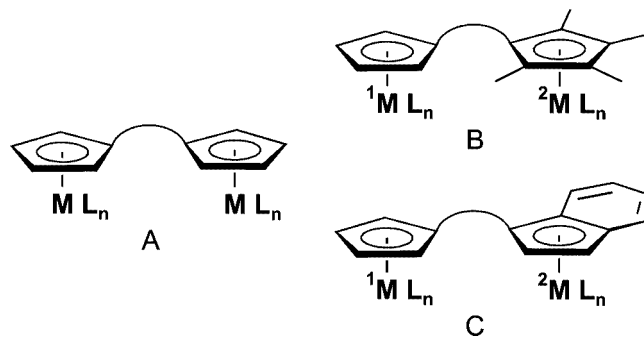


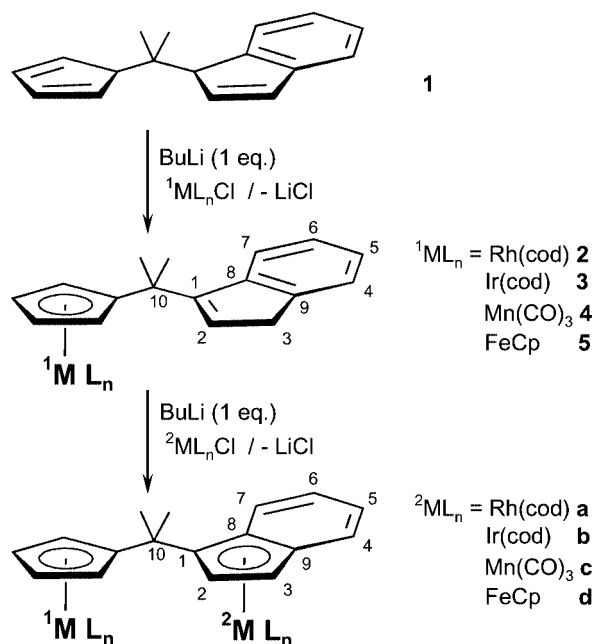
Figure 1

complex fragment proceeds at all Cp rings with almost the same rate, independent of whether the other Cp ring in the same ligand has already been metallated. Therefore the reaction with only one equivalent of reagent ends up usually with a mixture of the mono- and the homobinuclear products.

To overcome this problem, an unsymmetric ligand has been introduced and bimetallic complexes of type B have been obtained [4]. Our work follows a different route by replacing one of the Cp rings with an indenyl system [5], which leads to complexes of type C. This adds an interesting aspect to the reactivity of these compounds in catalytic reactions due to the well known “indenyl” effect which stands for the easy change from η^5 to η^3 hapticity [6]. The acidity of both ring systems in the ligand precursor **1** is so

* Dr. P. Escarpa Gaede
Technische Universität Berlin
Institut für Chemie, Sekr. C2
Straße des 17. Juni 135
D-10623 Berlin (Germany)
Fax: 49 30 3142 1106; Tel: 49 30 3142 3740
E-mail: Escarpa@chem.tu-berlin.de

Supporting information for this article is available on the WWW under <http://www.wiley-vch.de/home/zaac> or from the author.



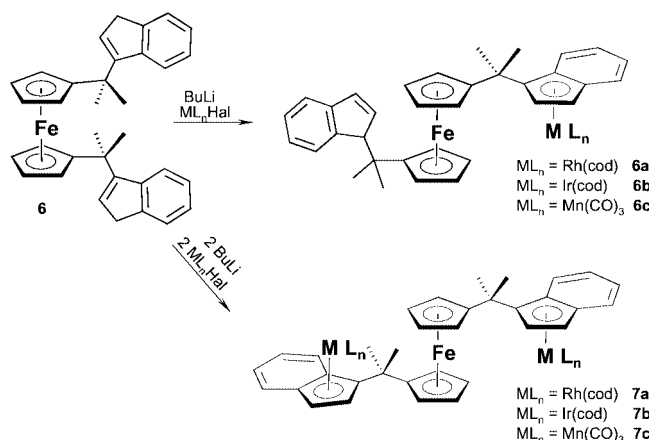
Scheme 1 Stepwise synthesis to obtain the heterobimetallic complexes **2a** to **5d** with numbering scheme for the NMR data.

different that the deprotonation is exclusively found at the Cp ring and heterobimetallic compounds can be obtained in a stepwise synthesis shown in scheme 1.

Results and Discussion

The length of the linker between the two five membered rings controls the strength of the steric and electronic interaction in these bimetallic complexes. A short bridging group keeps both metal complex fragments in close proximity, which should enhance intermetallic interaction. For this reason we choose the dimethylcarbon group as the linker between the two five membered rings to synthesize and investigate complexes of type C. This ligand system had been introduced to the syntheses of mono- [7], homobimetallic [8] and of some heterobimetallic complexes [9]. We have expanded the group of heterobimetallic compounds with this ligand by synthesizing the complexes [$^1\text{ML}_n(\text{C}_5\text{H}_4)\text{CMe}_2(\text{C}_9\text{H}_6)(^2\text{ML}_n)$] (**2a-5d**) with combinations of the metal complex fragments $^1\text{ML}_n$, $^2\text{ML}_n = \text{Rh}(\text{cod})^1$, $\text{Ir}(\text{cod})$, $\text{Mn}(\text{CO})_3$ and FeCp according to scheme 1. In all cases, the reaction proceeds with high selectivity and the products were obtained in good yields. Only for the synthesis of [$\text{Mn}(\text{CO})_3(\text{C}_5\text{H}_4)\text{CMe}_2(\text{C}_9\text{H}_6)\text{Mn}(\text{CO})_3$] (**4c**) from the dilithio salt and two equivalents of [$\text{Mn}(\text{CO})_5\text{Br}$], fore side products were detected by MS. These compounds were identified as [$\text{Mn}_2(\text{CO})_{10}$], the mononuclear species [$\text{Mn}(\text{CO})_3(\text{C}_5\text{H}_4)\text{CMe}_2(\text{C}_9\text{H}_7)$] (**4**) and two species giving molecular ions at $m/z = 580$ and 718 ,

¹⁾ cod = cyclooctadiene (C_8H_{12})



Scheme 2 Syntheses of the complexes **6a-c** and **7a-c**.

corresponding to complexes with coupled ligands like [$\text{Mn}(\text{CO})_3(\eta^5\text{-C}_5\text{H}_4)\text{CMe}_2(\text{C}_9\text{H}_6)(\text{C}_9\text{H}_6)\text{CMe}_2(\text{C}_5\text{H}_5)$] or [$\text{Mn}(\text{CO})_3(\eta^5\text{-C}_5\text{H}_4)\text{CMe}_2(\text{C}_9\text{H}_6)(\text{C}_5\text{H}_4)\text{CMe}_2(\text{C}_9\text{H}_7)$] and [$\text{Mn}(\text{CO})_3(\eta^5\text{-C}_5\text{H}_4)\text{CMe}_2(\text{C}_9\text{H}_6)(\text{C}_9\text{H}_6)\text{CMe}_2(\eta^5\text{-C}_5\text{H}_4)\text{Mn}(\text{CO})_3$], respectively. The coupling of olefin ligands in this kind of metathesis reaction is typical for manganese described in the literature [10]. The separation of this mixture by column chromatography was only partly successful.

We have recently reported the synthesis of the ferrocene derivative **6**, which can be obtained from monolithiated **1** and FeCl_2 [11]. Further deprotonation and metallation steps at the indenyl rings lead to the heterobimetallic species **6a** and **7a** with one or two additional rhodium cyclooctadiene (cod) fragments coordinated to the indenyl parts of the ligands [11]. Due to the equivalence of both indenyl substitutions at the ferrocene derivative **6**, we found the binuclear and the trinuclear species **6a** and **7a** in the product mixture including some starting material, when **6** reacted with only one equivalent of base and metal reagent. The compounds were separated by column chromatography. We extended this synthesis to introduce the metal moieties $\text{Ir}(\text{cod})$ and $\text{Mn}(\text{CO})_3$ instead of the $\text{Rh}(\text{cod})$ fragments and synthesized the complexes **6b**, **6c**, **7b** and **7c**, respectively (see scheme 2). Again, compound **7c** could not be isolated with satisfying purity because of side products formed in the reaction of a dilithio salt and [$\text{Mn}(\text{CO})_5\text{Br}$], as discussed above.

All synthesized compounds were characterized by MS, ^1H - and ^{13}C -NMR spectroscopy (see experimental section, the numbering of the atoms corresponds to that in figure 1).

Crystallographic studies

Single crystals of the complexes **3a**, **3b** and **5c** were obtained by slow evaporation from an diethyl ether solution at 4°C . Figure 2 shows the molecular structures of these three compounds, Table 1 gives the crystallographic data. Selected bond distances and interplanar angles are listed in Table 2 and 3, respectively.

Table 1 Crystallographic data

	5c	3a	3b
<i>Crystal parameters</i>			
Chem. formula	C ₂₅ H ₂₁ FeMnO ₃	C ₃₃ H ₄₀ RhIr	C ₃₃ H ₄₀ Ir ₂
Fw /g mol ⁻¹	480.21	731.76	821.05
Crystal system	monoclinic	triclinic	triclinic
Space group	C2/c (No. 15)	P $\bar{1}$ (No. 2)	P $\bar{1}$ (No. 2)
<i>a</i> /Å	18.4858(3)	7.09700(10)	7.09700(10)
<i>b</i> /Å	7.36210(10)	13.13110(10)	13.13110(10)
<i>c</i> /Å	30.8651(4)	14.4778(2)	14.4778(2)
α /°	90	89.8590(10)	89.8590(10)
β /°	92.1830(10)	82.5020(10)	82.5020(10)
γ /°	90	84.0630(10)	84.0630(10)
Volume /Å ³	4197.52(10)	1330.41(3)	1330.41(3)
<i>Z</i>	8	2	2
<i>D</i> (calc.) /g cm ⁻³	1.520	1.827	2.050
<i>F</i> (000)	1968	720	784
μ (Mo K α) /mm ⁻¹	1.317	5.637	10.013
<i>Data collection</i>			
2 θ range	4.48–50.0	3.12–55.0	2.84–50.0
Index range	–21 ≤ <i>h</i> ≤ 19, –8 ≤ <i>k</i> ≤ 8, –36 ≤ <i>l</i> ≤ 31	–9 ≤ <i>h</i> ≤ 5, –17 ≤ <i>k</i> ≤ 17, –18 ≤ <i>l</i> ≤ 17	–8 ≤ <i>h</i> ≤ 8, –15 ≤ <i>k</i> ≤ 15, –17 ≤ <i>l</i> ≤ 13
Data	12477	10243	8303
Indpt. obs. rflns.	3675	6063	4633
<i>R</i> _(int)	0.0584	0.0334	0.0466
Indpt. rflns.	3675	6063	4633
Parameters	271	319	318
<i>Refinement</i>			
$\Delta(\rho)$ /e·Å ⁻³	0.257 / –0.614	1.961 / –1.138	1.556 / –2.801
<i>T</i> _{max}	0.792039	0.297834	0.564153
<i>T</i> _{min}	0.457381	0.136212	0.241083
GOF	1.096	1.013	0.989
<i>R</i> ^a [%]	4.57 (5.97) ^b	3.18 (4.03) ^b	4.14 (5.65) ^b
<i>wR</i> ₂ ^a [%]	9.99 (10.59) ^b	7.62 (8.05) ^b	9.76 (10.41) ^b

^a) $R = \sum ||F_o| - |F_c|| / \sum |F_o|$, $wR_2 = [\sum (w(F_o^2 - F_c^2)^2) / \sum (w(F_o^2))]^{1/2}$, $[F_o > 4\sigma(F_o)]$.

^b) based on all data.

Crystallographic data for the structures have been deposited with the Cambridge Crystallographic Data Centre, CCDC231311–231313. Copies of the data can be obtained free of charge on application to The Director, CCDC, 12 Union Road, Cambridge, CB2 1EZ, UK (Fax: int. code+(1223)336-033; e-mail for inquiry: fileserv@ccdc.cam.ac.uk).

Due to the small difference in the atom radius between rhodium and iridium, the structures of the molecules **3a** and **3b** are isostructural and isotopic, which means even the cell dimensions are identical in all three structures. The metal atoms are η^5 -coordinated to the five membered ring in the Cp or in the indenyl part of the bridging ligand. The tendency to a η^3 displacement of the metal atom at the indenyl system is reflected in the difference of bond distances to C1 and C6 in relation to C7, C8 and C9. This elongation of the metal carbon bond lengths is obtained²⁾ to 5.2, 5.3 and 2.4 % for **3a**, **3b** and **5c**, respectively. The hinge angle given by the plane angle of the allyl system (C7, C8 and C9) to the ene-system (C7, C6, C1 and C9) is a further marker for this displacement. The largest angle is found for complex **3a** (7.8°) followed by 5.6° for **3b** and only 3.6° for **5c**. Most likely because of some steric interaction of the metal complex fragment with the two methyl groups of the bridging

²⁾ calculated from the quotient of the middle bond lengths: $1 - [1/2(M-C1 + M-C6) / 1/3(M-C7 + M-C8 + M-C9)]$

Table 2 Selected bond lengths / Å in [¹ML_n(η^5 -C₅H₄)CMe₂(η^5 -C₉H₆)²ML_n].

	3b	3a	5c
M(1)–C(11)	2.298(4)	2.31(1)	2.052(3)
M(1)–C(12)	2.198(5)	2.19(1)	2.044(3)
M(1)–C(13)	2.223(5)	2.23(1)	2.031(4)
M(1)–C(14)	2.247(5)	2.241(13)	2.032(4)
M(1)–C(15)	2.267(5)	2.28(1)	2.040(3)
M(1)–C(Cp) ^{a)}	2.246(5)	2.252(13)	2.040(4)
M(1)–C(L _n) ^{b)}	2.109(5)	2.11(1)	2.039(4)
M(2)–C(7)	2.207(5)	2.228(9)	2.132(4)
M(2)–C(8)	2.252(5)	2.234(9)	2.142(3)
M(2)–C(9)	2.263(4)	2.260(9)	2.165(3)
M(2)–C(6)	2.344(4)	2.348(9)	2.190(3)
M(2)–C(1)	2.374(4)	2.351(8)	2.209(3)
M(2)–C(L _n) ^{b)}	2.142(5)	2.14(1)	1.794(4)
C(CO)–O(CO) ^{a)}			1.147(4)
C(1)–C(2)	1.405(7)	1.428(13)	1.427(5)
C(1)–C(6)	1.434(6)	1.422(13)	1.435(5)
C(1)–C(9)	1.456(6)	1.459(13)	1.459(5)
C(2)–C(3)	1.381(8)	1.393(18)	1.364(6)
C(3)–C(4)	1.42(1)	1.37(2)	1.417(8)
C(4)–C(5)	1.34(1)	1.36(2)	1.349(7)
C(5)–C(6)	1.426(8)	1.401(16)	1.427(5)
C(6)–C(7)	1.432(8)	1.422(15)	1.431(6)
C(7)–C(8)	1.409(7)	1.410(15)	1.416(5)
C(8)–C(9)	1.419(6)	1.421(13)	1.426(5)
C(9)–C(10)	1.548(6)	1.553(14)	1.533(5)
C(10)–C(16)	1.542(8)	1.513(15)	1.528(5)
C(10)–C(17)	1.517(7)	1.507(14)	1.538(5)
C(10)–C(11)	1.539(6)	1.517(13)	1.521(4)
C(11)–C(12)	1.402(8)	1.464(15)	1.426(5)
C(11)–C(15)	1.417(8)	1.417(16)	1.431(5)
C(12)–C(13)	1.436(9)	1.44(2)	1.423(5)
C(13)–C(14)	1.37(1)	1.39(2)	1.400(6)
C(14)–C(15)	1.414(8)	1.416(16)	1.430(5)

^a) average value, ^b) average value L_n stands for the coligand cod or CO.

ligand, the distance between the metal atom and the quar-terial carbon atom C9 is always longer than the corresponding bond lengths to C7 or C8. Comparing the three structures, the main difference is found in the conformation of the bridging ligand. The dihedral angle ϕ (C11–C10–C9–C1) is the characteristic parameter for the orientation of both coordination planes in these molecules, and detected as

Table 3 Interplanar angle / ° and distance of the metal atom to the plane in [¹ML_n(η^5 -C₅H₄)CMe₂(η^5 -C₉H₆)²ML_n].

	3b	3a	5c
∠ Pl 1–Pl 2	89.1 (0.4)	89.8 (0.2)	76.7 (0.1)
∠ Pl 3–Pl 4	5.6 (1.3)	7.8 (0.6)	3.6 (0.5)
∠ Pl 1–Pl 5	5.1 (0.4)	4.8 (0.2)	3.1 (0.3)
∠ Pl 2–Pl 6	2.6 (0.7)	3.8 (0.4)	
Pl 1 – M(1)	1.896(5)	1.899(2)	1.642(1)
Pl 2 – M(2)	1.931(3)	1.932(2)	1.792(1)
Pl 5 – M(1)	1.453(5)	1.449(2)	1.649(2)
Pl 6 – M(2)	1.460(4)	1.467(2)	
Pl 1: [C11–C15]			
Pl 2: [C1–C9]			
Pl 3: [C7–C9]			
Pl 4: [C1;C6;C7;C9]			
Pl 5: [¹ L _n]	C18;C19;C22;C23	C18;C19;C22;C23	C18 – C22
Pl 6: [² L _n]	C26;C27;C30;C31	C26;C27;C30;C31	

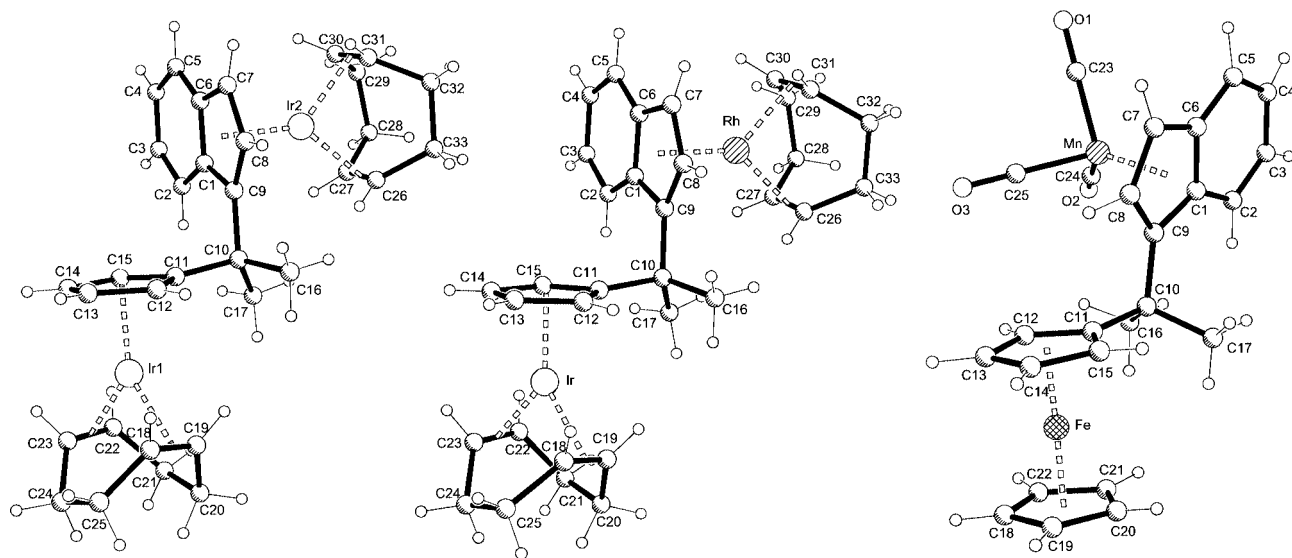


Figure 2 Molecular structure of **3a**, **3b** and **5c**.

75.7°, 75.2° and 177.9° for **3a**, **3b** and **5c**, respectively. In other known structures with the same bridging ligand dihedral angles of 177.3° (**5a**) [11], 172.9° [$(\eta^5\text{-C}_5\text{H}_4)\text{CMe}_2(\eta^5\text{-C}_9\text{H}_6)\text{Rh}_2(\text{C}_2\text{H}_4)_4$] and 75.9° (**3a**) [7a] are found. The rotation around the C9–C10 bond thus gives rise to two rotamers which can be classified as anti ($\varphi \approx 180^\circ$) or gauche ($\varphi \approx \pm 75^\circ$). It is not obvious why different compounds have solid state structures which belong to different rotamer classes. It would be interesting to know whether this is mainly a crystal packing effect or whether the propensity for different rotamers is already developed for isolated (i.e. gas phase) molecules.

Theoretical calculations

We applied quantum chemical density functional calculations to compute the energy profile associated with a rotation around C9–C10. We chose the two rhodium compounds **2a** and **5a** as representatives for the gauche and the anti class, respectively. First a geometry optimization was performed, starting from the coordinates found in the crystal. This step essentially moves the hydrogen atoms to their correct positions. Starting from this geometry, the torsion angle $\varphi(\text{C1-C9-C10-C11})$ was fixed in steps of 10° , relaxing all other internal coordinates to their optimal values. Figure 2 shows the resulting energy profiles for the two compounds.

There are only small differences between the two curves which are mostly caused by variable conformations in the cyclooctadiene rings than by intramolecular interactions between the two molecule parts. Within a tolerance of 1 kJ/mol, two minima are found with the same energy at $60 - 70^\circ$ (conformation 1 = gauche) and $170 - 180^\circ$ (conformation 2 = anti). The third minimum at 320° shows a higher energy level, the difference is marked by 4 kJ/mol. This must be attributed to the second gauche conformation

of the two metal complex fragments. The conformations found in the molecular structures conforms to the resulted structures at the minima 1 and 2. The absolute rotation barrier is 23 kJ/mol calculatedly, but there are two other maxima of a little bit lower energy barrier. Over all, the curves are very similar to that of butane, only the energy barriers are a little bit higher as for the alkane. The hump at 280° is caused by steric interaction of the indenyl metal complex fragment with the Cp ring, because it locates over the five membered ring at this torsion angle.

According to the result, there is no energetic difference between both conformations 1 and 2 in the gas phase. On the other hand, no intramolecular interactions can be found in the solid state. We presume the preference for the chosen conformation in the crystal structure of each compound is only controlled by molecular packing in the crystal. From the energetic height of the rotations barrier we can conclude that the complexes are very flexible and that the metal-metal distance can be modified easily in solution. That is important, if both metals act in concert with a substrate coordinated to both metals.

Electrochemical measurements

The electronic interaction between two metal atoms in a ligand bridged complex can be measured by cyclic voltammetry (CV). This has been achieved for symmetric compounds in the literature, mostly for bisferrocenyl species [12]. In such a CV, two signals are shown, each indicating a single electron transfer. The potential difference between these two one-electron-steps corresponds to the strength of the intermetallic interaction. Depending on the bridging atoms between the two ferrocenyl moieties, ΔE values were reported up to 800 mV for a totally delocalisation of the positive charge in the mixed valence complex. Robin and Day [13] introduced a classification into three groups of

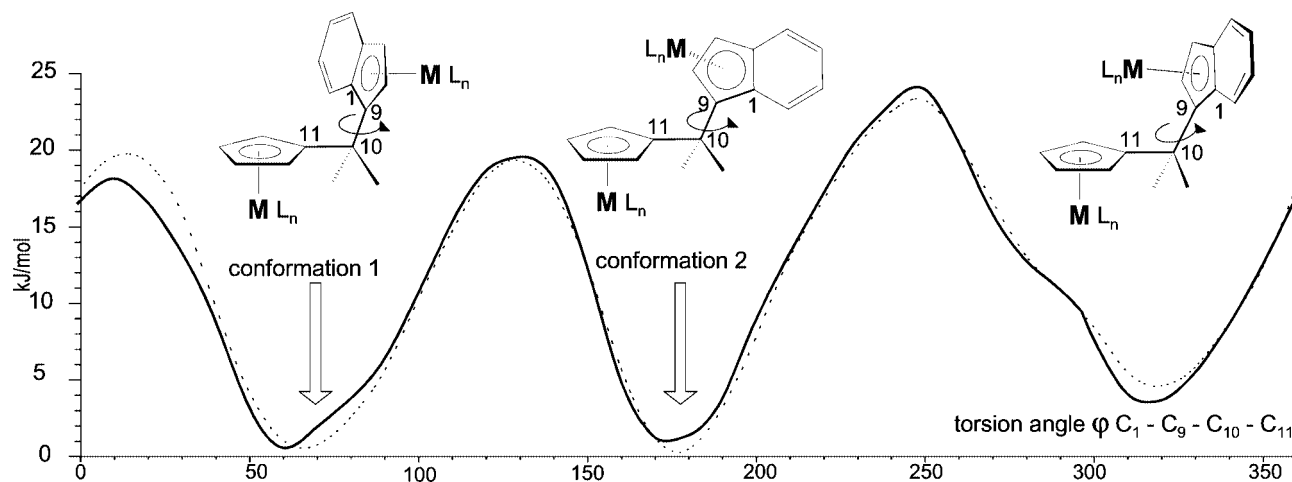


Figure 3 Energy of the complexes **2a** (full line) and **5a** (dotted line) correlated to the torsion angle ϕ C1-C9-C10-C11.

compounds: class I shows none or only weak interaction of the metal centers corresponding to ΔE values of 0 – 200 mV, class III species are characterized by a strong π -delocalisation in the bridging ligand with ΔE values larger than 500 mV. Complexes showing values between these extremes possess only partial delocalisation of the unpaired electron over the two metal moieties. The potential difference also weakly depends on the solvent, the supporting electrolyte [14] and the nature of the metals themselves, if the iron atoms were substituted, for instance, by nickel or cobalt atoms. For a C₁ bridging moiety as in the compounds discussed in this paper, ΔE values between 100 and 150 mV are expected [12].

In contrast to the symmetric complexes described in the literature, the homobimetallic species **2a**, **3b**, **4c** and **5d** show two steps in the CV even in the absence of any electronic interaction due to the unsymmetric structure of the complexes and the electronic dissimilarity of the Cp and the indenyl system. Therefore, we can not merely look at the ΔE value in the bimetallic complexes, but compare the potential values obtained from the bimetallic compound with those of the corresponding mononuclear Cp or indenyl species, respectively (Table 4, all values were referred against ferrocene as external standard). This gives us a potential shift $\Delta E(M)$ for each metal complex fragment in the bimetallic compound. The difference between these two $\Delta E(M)$ values is comparable to the original ΔE in symmetric complexes. This can be illustrated in Figure 4 on the example of compound **5d**, where its CV is shown beside those obtained from ferrocene and [(Ind)FeCp] (Ind = Indenyl, C₉H₇). The first oxidation wave of **5d** at –140 mV can be attributed to the iron center within the indenyl part, the second at 125 mV to that on the Cp part of the linked ligand. The two redox waves are thus separated by 265 mV. Compared to the mononuclear reference compounds [(Ind)FeCp] and ferrocene, the first oxidation is shifted towards lower potential by 65 mV, while the second is shifted by 70 mV to higher potential. This totally gives a separation shift of 135 mV for the bimetallic iron species, which is in good

agreement with the expected value of 100 – 150 mV. Similar results were obtained looking at the half potentials $E_{1/2}$.

The reversibility of the two redox steps in **5d** is comparable with that in ferrocene indicated by slightly larger potential differences ΔE^R between the corresponding oxidative and reductive current maxima. This fact is very useful in the case when the iron oxidation is superposed by the irreversible oxidation of another metal complex fragment. In this case the reductive peak can be used to calculate $E_{1/2}$ for the iron moiety under the assumption that the ΔE^R values are comparable. Generally we have observed even in water based systems relatively high ΔE^R values compared to the theoretical value of 58 mV. This is deduced from the missing compensation of faraday current with the Metrohm potentiostat that has been used.

The potentials of the mononuclear complexes **2** to **6** are listed in table 4. The unsubstituted Cp or indenyl species are used as references for the shift determination $\Delta E(M)$ in the bimetallic compounds **2a** to **7b**, which are given together with their measured oxidation potentials in table 5. The values in this table refer to the $E_{1/2}$ for the iron containing moieties, and to E_{\max} for the irreversible oxidations of all other metal complex fragments. The values ΔE_{net} in the last

Table 4 $E_{1/2}$ and potential at the current maxim measured with 50 mV/s.

complex	$E_{1/2}$ / mV	E_{\max} / mV
CpRh(cod)		75
(Ind)Rh(cod)		120
2		60
CpIr(cod)		180
(Ind)Ir(cod)		190
3		180
CpMn(CO) ₃		865
(Ind)Mn(CO) ₃		780
4		925
Cp ₂ Fe	0	55
(Ind)FeCp	–130	–75
5	–15	55
6	–10	55

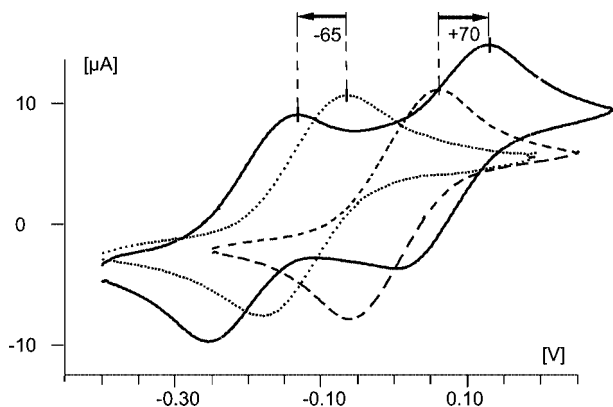


Figure 4 CV of **5d** (full line), ferrocene (broken line) and (Ind)FeCp (dotted line) in CH_2Cl_2 at 100 mV/s.

column is calculated as the differences of both $\Delta E(\text{M})$ values, where $\Delta E_{\text{net}} = \Delta E(^2\text{M}) - \Delta E(^1\text{M})$, if the metal atom ^1M is oxidized at lower potential as ^2M , or $\Delta E_{\text{net}} = \Delta E(^1\text{M}) - \Delta E(^2\text{M})$ in the opposite case. ΔE_{net} represents the total drifts of both redox steps; a positive value is attributed to an increasing separation of both redox waves as expected, while a negative difference indicates a decreasing separation.

A group of complexes shows the expected value around 130 mV for ΔE_{net} , but much higher values were observed for species **4a** and **6c**. A second group of compounds, especially those with an iridium fragment, shows significantly smaller differences around 65 to 85 mV. This can be attributed to the metal influence known from the literature by various peak separations ΔE for different bismetallocenes with the same bridging ligand [15].

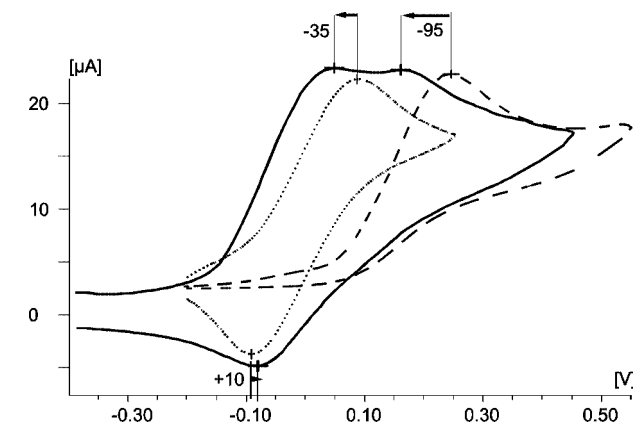
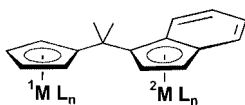


Figure 5 CV of **6b** (full line), **6** (dotted line) and (Ind)Ir(cod) (broken line) in CH_2Cl_2 at 100 mV/s.

For some complexes, a negative ΔE_{net} was obtained, which means that the separation of the peaks decreases. Thereby both peaks must not necessarily move towards each other. Some compounds show shifts to lower potential for both redox steps but while the second shift is much larger than the first one, which also results in a negative ΔE_{net} . Figure 5 demonstrates this phenomenon for **6b**. Both metal atoms in **6b** were oxidized at a lower potential as the corresponding mononuclear species. The shift to lower potential for the iridium centered oxidation is 50 mV higher than for the iron atom. This unusual behaviour was found for a number of complexes mainly when a ferrocenyl and a rhodium or iridium fragment are involved. For interpretation, we suggest a mechanism with an intramolecular catalytic oxidation step (scheme 3). After the first oxidation the positive charge is transferred to the second metal atom. This occurs at a lower potential level than normally required to oxidize the second metal atom. The first metal atom is oxidized again as soon as the second metal atom transferred the electron to it. This phenomenon of catalytic oxidation is well known for bimolecular systems [16] but is to our knowledge unprecedented for intramolecular processes.

We point out that intramolecular charge transfer has been well established in the literature [17]. For example *T.J.J. Müller* explained the irreversibility of the chromium oxidation in linked ferrocenyl phenyl tricarbonyl chromium complexes $[\text{Fc-X}-(\text{C}_6\text{H}_5)\text{Cr}(\text{CO})_3]$ in contrast to the reversible oxidation in $[(\text{C}_6\text{H}_5)\text{Cr}(\text{CO})_3]$ by such intramolecular positive charge transfer from the iron to the chromium atom [17e]. The other example has been given by *Ceccon* et al. with a ferrocenyl indenyl rhodium dicarbonyl complex [18]. These two examples show that a ferrocenium cation can interact with a neutral metal complex fragment, if both are relatively close to each other. The tendency to transfer one electron to the ferrocenium part in the molecule is very strong, if electron rich metal complex fragments with rho-

Table 5 Redox potential for compounds **2a** to **7b** and their potential shift compared to their correspondent Cp or indenyl complex with a scan rate of 50 mV/s.

					
	$E(^1\text{M})$	$E(^2\text{M})$	$\Delta E(^1\text{M})$	$\Delta E(^2\text{M})$	ΔE_{net}
2a	110	115	+35	-10	-45 ^{a)}
2b	45	165	-30	-25	+5 ^{a)}
2c	45	875	-30	+95	+125 ^{a)}
2d	160	-175	+85	-45	+130 ^{b)}
3a	215	30	+35	-90	+125 ^{b)}
3b	~125	~220	-55	+30	+85 ^{a)}
3c	245	925	+65	+145	+80 ^{a)}
3d	155	-220	-25	-90	+65 ^{b)}
4a	960	30	+95	-90	+185 ^{b)}
4b	~870	245	+5	+55	-50 ^{b)}
4d	995	-140	+130	-10	+140 ^{b)}
5a	40	105	+40	-15	-55 ^{a)}
5b	-20	155	-20	-35	-15 ^{a)}
5c	-40	885	-40	+105	+145 ^{a)}
5d	60	-200	+60	-70	+130 ^{b)}
6a	~-10	85	-10	-35	-25 ^{a)}
6b	-35	105	-35	-85	-50 ^{a)}
6c	10	1045	+10	+265	+255 ^{a)}
7a	~-5	45	-10	-75	-65 ^{a)}
7b	~-140	105	-140	-85	+55 ^{a)}

^{a)} $\Delta E(^2\text{M}) - \Delta E(^1\text{M})$

^{b)} $\Delta E(^1\text{M}) - \Delta E(^2\text{M})$

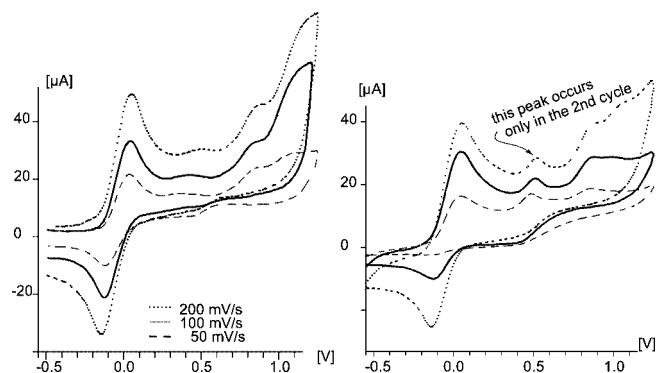
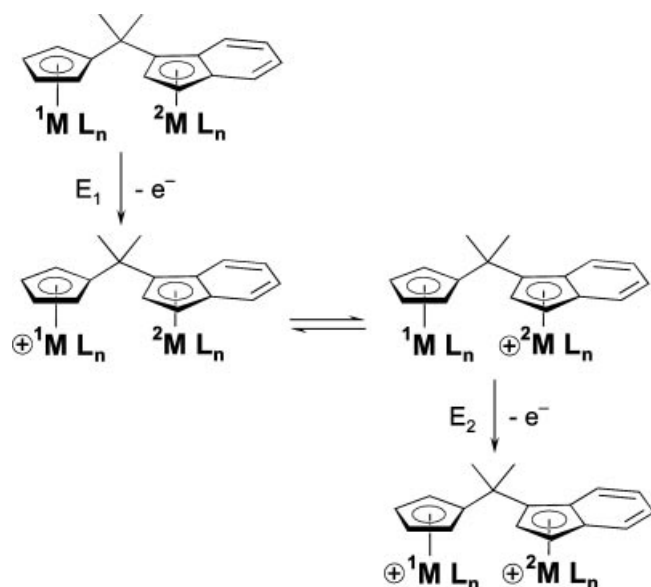


Figure 6 first (left) and second (right) cycle in the CV of **5c** in CH_2Cl_2 at different scan rates.

dium or iridium are involved, which have similar redox potentials as ferrocene. We could not observe such effects for the coordination isomers, where the metal complex fragments are exchanged at the two ligand parts and the iron is bound to the indenyl ring.

Beside this investigations to the intermetallic interactions in the bimetallic compounds some other interesting aspects have been observed in the cyclic voltammetry of compound **5c**, if the first and second cycle were compared with each other (figure 6). The redox signal of the ferrocene part of the molecule is clearly shown at ca. -0.04 V. In contrast, the irreversible oxidation of the $\text{Mn}(\text{CO})_3$ moiety at 0.90 V forming the species $\mathbf{5c}_1^{2+}$ by an electron transfer followed by a chemical reaction (EC mechanism) is indicated only by a shoulder in the CV. In the first cycle the oxidation of iron appeared to be reversible (Fig. 6, left panel). However, in a second run, the wave for the iron reduction decreases comparing to the corresponding oxidative wave, which indicates reduced reversibility. This loss of reversibility increases with slower scan rates. If the potential is only run to 0.6 V



Scheme 3 mechanism of the catalytical intramolecular oxidation.

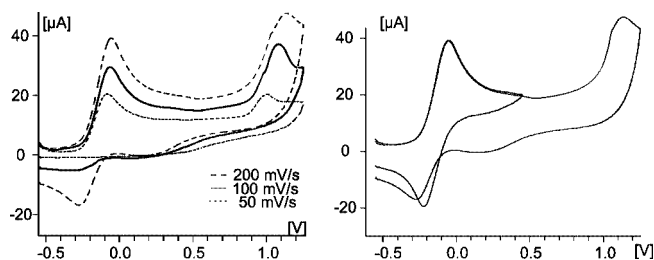
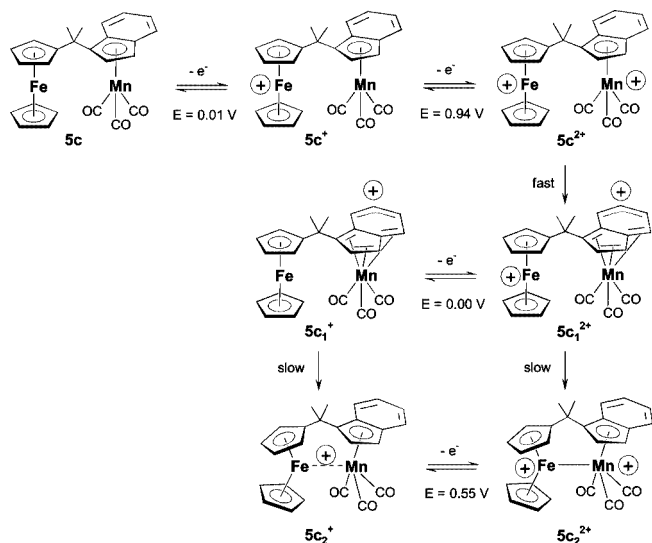


Figure 7 left: first circle in the CV of **4d** in CH_2Cl_2 at different scan rates. right: CV of **4d** with different scan ranges at 200 mV/s.

without reaching the value where the manganese becomes oxidized, reversibility sustained even after ten cycles. Therefore, a second chemical reaction forming the compound $\mathbf{5c}_2^{2+}$ must be induced from the manganese center then the iron moiety of the molecule is involved. This transformation is slow compared to the first reaction, which makes the manganese oxidation characteristically irreversible and does not involve the ferrocenyl part of the molecule. Furthermore, a new product wave for oxidation at 0.50 V occurs in the second cycle together with a small corresponding cathodic step at the back sweep. Such a product wave is not observed from any other manganese compounds. The intensity of this signal does not change with the scan rate as usual. In relation to the other signals, this peak increases with slower scan rates. We suppose that this redox signal belongs to the product compound $\mathbf{5c}_2^{2+}/\mathbf{5c}_2^{2+}$, which is formed by the slow second chemical reaction as we have discussed above. $\mathbf{5c}_2^{2+}$ is an unstable species and precipitates on the surface of the electrode preventing any further redox process on the coated surface. For this reason, we can't prove whether the second chemical reaction starts from the bicationic species $\mathbf{5c}_1^{2+}$ or the monocationic $\mathbf{5c}_1^{+}$ or even from both. A similar behavior is found for the related compound **6c**.

Looking at the CV of the coordination isomer **4d** of compound **5c**, where the metal complex fragments are exchanged between the Cp and indenyl part of the ligand (figure 7), the intensity of the iron reduction peak in the first circle already decreases with the scan rate. This must be interpreted as a increasing reaction rate in the second chemical step. This interpretation is furthermore supported by the absence of the new oxidation wave at around 0.5 V in the second cycle. Only the small hump at the back sweep of the first cycle indicates the appearance of the analogue intermediate $\mathbf{4d}_2^{2+}$, which has also a shorter life time as its isomer $\mathbf{5c}_2^{2+}$. The change in reversibility of the iron oxidation is also demonstrated in dependence of the reversal potential in that figure 7.

In analogy to the mechanism discussed by *Ceccon et al.* [18] for the mentioned similar compound 2-ferrocenyl-indenyl-rhodiumdicarbonyl we propose the reaction scheme shown in scheme 4. This phenomenon is restricted to mixed iron manganese compounds and no such observations can be done for the other $\text{Mn}(\text{CO})_3$ complexes **2c**, **3c**, **4a** and **4b**.



Scheme 4 Reaction scheme for the electrochemical redox behavior of **5c**.

Conclusion

For the synthesis of heterobimetallic complexes the olefin $(C_5H_5)CMe_2(C_9H_7)$ is a very useful compound as a bridging ligand, because the stepwise deprotonation of the five membered rings is very selective. A further advantage of this bridging ligand system is its easy rotation around the C-C-bonds in the C_1 -bridge, which impart a good flexibility in conformation of both metal moieties to each other. This is important for catalytic reactions where both metal complex fragments interact with the substrate in a concerted fashion. A number of bimetallic complexes have been synthesized and characterized with the metal complex fragments Rh(cod), Ir(cod), Mn(CO)₃ and FeCp. Conformation analysis for two different complexes has given the same minimum in energy for the anti and one gauche conformation, which both are found in the solid state.

The electronic intermetallic interaction in these complexes has been investigated by electrochemical measurements. In general we presume that a weak electronic intermetallic communication can be established in all compounds. The effect of this interaction varies in the cyclic voltammograms of the heterobimetallic complexes. Some species show an increase of the potential separation (positive ΔE), which we call the “normal effect”, but some compounds behave opposite to that (negative ΔE), named the “unusual effect”. This “unusual effect” is interpreted as an intramolecular catalytic oxidation. This is the first case in which such an intramolecular catalytic oxidation is observed.

Experimental Section

Reactions were carried out under nitrogen using conventional Schlenk techniques. All solvents were dried over sodium / benzophenone and freshly distilled prior to use. The NMR spectra were

recorded with the Bruker ARX 200 spectrometer in C_6D_6 (1H : 200.1 MHz, ^{13}C : 50.3 MHz). $[(cod)RhCl]_2$ [19], $[(cod)IrCl]_2$ [19], $[Mn(CO)_3Br]$ [20], $[(fluorene)FeCp]PF_6$ [21], $(C_5H_5)CMe_2(C_9H_7)$ [5] and the complexes **2**, **4**, **2a** [7], and **6**, **6a**, **7a** [11] were prepared by literature methods. Mass spectra (EI, 70 eV) were recorded with a modified Varian MAT 311A. The X-ray diffraction structural analyses were performed with Mo K α radiation ($\lambda = 0.71073$ Å, graphite monochromator) at 293 K using the Siemens SMART CCD area detector diffractometer. All crystal structures were solved by using the direct method (SHELXS86) and subsequently refined by full-matrix least-squares method's (SHELXL93 [22]). For all structures the final absorption correction was done by SADABS. The positions of all hydrogen atoms were calculated with a fixed thermal parameter. The data for structure refinement of **3b**, **3a** and **5c** are listed in table 1, selected bond lengths are summarized in table 2.

Quantum chemical density functional calculations were performed with the TURBOMOLE [23] (version 5.5) suite of programs. The calculations were done with a gradient-corrected exchange-correlation functional (BP86), following the work of Becke [24] and Perdew [25]. The matrix elements of the Hartree potential were obtained by a density fitting (also known as RI) procedure [26]. Polarised basis sets of triple-zeta quality in the valence shell (TZVP [27]) were used for the carbon and metal atoms, while the hydrogen atoms carried polarized double-zeta (SVP [28]) basis sets. For the Rh atoms, the innermost 28 electrons were replaced by a small-core scalar-relativistic effective core potential [29].

The electrochemical measurements were performed on a Metrohm VA693 with a three-electrode configuration in methylene chloride with scan rates from 50 to 200 mV/s. The supporting electrolyte was tetrabutylammonium tetrafluoroborate (TBAB) 0.1 M. A Ag/AgCl/KCl_{aq} half cell was used as reference electrode, which was separated from the sample cell by a second integrated electrolyte (saturated LiCl in ethanol) to avoid large liquid junction and contamination of the non aqueous cell. A glass frit and a glass membrane separate the electrolytes from each other. A polished Platinum disk electrode with a 2 mm diameter was used as the working electrode, a Pt-wire as the auxiliary electrode. All potentials were referred to ferrocene-ferrocenium, the value for which was obtained by subsequent measurement under the same conditions.

Synthesis of $[(C_9H_7)CMe_2(\eta^5-C_5H_4)Ir(cod)]$ (3**):** 0.65 ml butyllithium (1.6 mol/l) were added to a solution of 220 mg (0.99 mmol) $(C_5H_5)CMe_2(C_9H_7)$ in 20 ml diethyl ether and stirred at room temperature. After 2 h a THF solution of 338 mg (0.5 mmol) $[Ir(cod)Cl]_2$ was added and the orange reaction mixture was stirred for another 2 hours. The solvent was removed *in vacuo*. The residue was filtered through a short column of Al_2O_3 . With hexane, 287 mg (0.55 mmol, 55 %) of $[(C_9H_7)CMe_2(\eta^5-C_5H_4)Ir(cod)]$ were isolated as a colorless solid. $M(C_{21}H_{25}Ir) = 521.71$ g/mol; C: 57.98 (calc. 57.55); H: 5.83 % (5.60) %.

NMR (C_6D_6) δ_H = 4.62 (2 H, t, $J(HH)$ 2 Hz, H_{Cp}), 4.90 (2 H, t, $J(HH)$ 2 Hz, H_{Cp}), 5.97 (1 H, t, $J(HH)$ 2.2 Hz, H_2), 2.99 (2 H, d, $J(HH)$ 2.2 Hz, H_3), 1.71 (6H, s, H_{Me}), 7.57 (1 H, d, $J(HH)$ 8 Hz, H_7), 7.19 (1 H, d, $J(HH)$ 8 Hz, H_6), 7.24 (1 H, m, H_5), 7.00 (1 H, m, H_4), 3.85 (4 H, br m, H_{cod}), 2.25 (4 H, m, H_{cod}), 1.98 (4 H, m, H_{cod}). δ_C = 153.0 (C_1), 145.8 (C_8), 144.1 (C_9), 127.5 (C_2), 126.0, 124.4, 124.2, 122.7, 113.2 (C_5H_4), 81.8 (2 C, C_5H_4), 81.0 (2 C, C_5H_4), 37.1 (C_3), 36.5 (C_{10}), 30.0 (2 C, C_{Me}), 46.5 (4 C, C_{cod}), 34.4 (4 C, C_{cod}). **MS** (120 °C, EI) m/z = 522 (M^+ , 100 %), 412 ($M-cod-H_2$, 20 %), 405 ($M-Ind-H_2$, 65 %), 363 ($M-CMe_2Ind-H_2$, 40 %).

Synthesis of $[(C_9H_7)CMe_2(\eta^5-C_5H_4)FeCp]$ (5**):** 220 mg (0.99 mmol) $(C_5H_5)CMe_2(C_9H_7)$ were dissolved in 20 ml THF in a 100 ml flask and deprotonated with 0.65 ml BuLi (1.6 mol/l) at room temperature. In another flask the “CpFe” reagent was pre-

pared from 430 mg (0.99 mmol) [CpFe(fluorene)]PF₆ and 0.65 ml BuLi in THF. After 1 h stirring, this blue THF solution was added at 0 °C to the yellow solution in the first flask and the resulting reaction mixture was refluxed for 16 h. The solvent was removed and the residue extracted with pentane / diethyl ether (1:1). Before the product was isolated by chromatography over a short column of Al₂O₃ with hexane, fluorene and ferrocene were removed by sublimation at 40 °C. 144 mg (0.42 mmol, 42 %) of [(C₉H₇)CMe₂(η⁵-C₅H₄)FeCp] were obtained as a yellow orange solid. M(C₂₂H₂₂Fe) = 342.26 g/mol; C: 77.41 (calc. 77.20); H: 6.55 (6.48) %.

NMR (C₆D₆) δ_H = 4.05 (2 H, t, J(HH) 2 Hz, C₅H₄), 3.96 (2 H, t, J(HH) 2 Hz, C₅H₄), 5.76 (1 H, t, J(HH) 2 Hz, H₂), 2.92 (2 H, d, J(HH) 2 Hz, H₃), 1.74 (6 H, s, H_{Me}), 7.64 (1 H, d, J(HH) 8 Hz, H₇), 7.24 (1 H, d, J(HH) 8 Hz, H₄), 7.20 (1 H, t, J(HH) 8 Hz, H₅), 7.05 (1 H, t, J(HH) 8 Hz, H₆), 4.06 (5 H, s, C_{Cp}). δ_C = 154.1 (C₁), 145.9 (C₈), 144.2 (C₉), 127.3 (C₂), 125.9, 124.3, 124.2, 122.6, 100.4 (C₅H₄), 67.2 (2 C, C₅H₄), 67.1 (2 C, C₅H₄), 36.9 (C₃), 36.2 (C₁₀), 28.2 (2 C, C_{Me}), 68.5 (5 C, C_{Cp}). **MS** (100 °C, EI) m/z = 342 (M⁺, 90 %), 227 (M–Ind, 100 %), 186 (C₂Fe, 15 %), 121 (M–CpCMe₂Ind, 20 %).

Synthesis of [Rh(cod)(η⁵-C₅H₄)CMe₂(η⁵-C₉H₆)Ir(cod)] (2b): 0.4 ml butyllithium (1.3 mol/l) were added to a solution of 253 mg (0.59 mmol) of **2** in 20 ml THF and stirred at room temperature. After 2 h stirring, 190 mg (0.28 mmol) [Ir(cod)Cl]₂ were added and stirred for another 8 hours. After removing the solvent, the reaction mixture was chromatographed on Al₂O₃. A small amount of educt was obtained first with pure hexane, before 331 mg (0.45 mmol, 78 %) of **2b** were isolated with a hexane / diethyl ether (1:1) mixture as a pale yellow solid. M(C₃₃H₄₀RhIr) = 731.79 g/mol; C: 53.88 (calc. 54.16); H: 5.32 (5.51) %.

NMR (C₆D₆) δ_H = 4.91 (2 H, m, C₅H₄), 4.65 (1 H, m, C₅H₄), 4.53 (1 H, m, C₅H₄), 5.78 (1 H, d, J(HH) 2.8 Hz, H₂), 4.72 (1 H, d, J(HH) 2.8 Hz, H₃), 1.80 (3 H, s, H_{Me}), 1.73 (3 H, s, H_{Me}), 7.42 (1 H, m, H₇), 7.16 – 7.0 (3 H, m, H_{4–6}), 3.99 (4 H, br m, H_{Rhcod}), 3.93 (4 H, br m, H_{Irircod}), 2.24 (8 H, m, H_{cod}), 1.96 – 1.70 (8 H, m, H_{cod}). δ_C = 123.5, 123.3, 121.8, 121.7, 120.8 (C₅H₄, J(RhC) 4 Hz), 109.6 (C₈), 108.9 (C₉), 101.7 (C₁), 86.0 (C₅H₄, J(RhC) 3.8 Hz), 85.9 (C₅H₄, J(RhC) 3.8 Hz), 85.5 (C₅H₄, J(RhC) 3.6 Hz), 84.5 (C₅H₄, J(RhC) 3.7 Hz), 84.8 (C₂), 69.5 (C₃), 36.6 (C₁₀), 31.5 (C_{Me}), 30.3 (C_{Me}), 63.0 (4C, J(RhC) 14 Hz, C_{Rhcod}), 32.9 (4C, C_{Rhcod}), 51.2 (2 C, C_{Irircod}), 50.9 (2 C, C_{Irircod}), 33.6 (2 C, C_{Irircod}), 32.9 (2 C, C_{Irircod}). **MS** (150 °C, EI) m/z = 732 (M⁺, 50 %), 622 (M–cod–H₂, 100 %), 415 ((Ind)Ir(cod)–H, 45 %), 317 (M–(Ind)Ir(cod), 34 %).

Synthesis of [Rh(cod)(η⁵-C₅H₄)CMe₂(η⁵-C₉H₆)Mn(CO)₃] (2c): 0.16 ml butyllithium (1.6 mol/l) were added to a solution of 110 mg (0.25 mmol) of **2** in 20 ml THF and stirred at room temperature. After 3 h stirring, 80 mg (0.29 mmol) [Mn(CO)₅Br] were added. The orange solution was stirred for another hour then refluxed for another 6 h. After changing the solvent to pentane / diethyl ether the reaction mixture was first filtered through Al₂O₃ to remove the by-product [Mn₂(CO)₁₀] and some unreacted starting material as the first two yellow bands. The third fraction was chromatographed again on a long column of Al₂O₃. 10 mg (0.0175 mmol, 7 %) of **2c** could be isolated as an orange solid with a hexane / benzene mixture. M(C₂₈H₂₈RhMnO₃) = 570.36 g/mol; C: 59.14 (calc. 58.96); H: 4.69 (4.95) %.

NMR (C₆D₆) δ_H = 4.98 (2 H, m, C₅H₄), 4.64 (1 H, m, C₅H₄), 4.60 (1 H, m, C₅H₄), 4.42 (1 H, d, J(HH) 2.4 Hz, H₂), 4.47 (1 H, d, J(HH) 2.4 Hz, H₃), 1.81 (3 H, s, H_{Me}), 1.76 (3 H, s, H_{Me}), 7.43 (1 H, d, J(HH) 8.4 Hz, H₇), 7.00 (1 H, d, J(HH) 8.4 Hz, H₄), 6.73 (1 H, t, J(HH) 8.4 Hz, H₆), 6.58 (1 H, t, J(HH) 8.4 Hz, H₅), 3.93 (4 H, br s, H_{Rhcod}), 2.23 (4 H, m, H_{cod}), 1.93 (4 H, m, H_{cod}). δ_C = 127.3, 126.5, 125.4, 124.9, 118.7 (C₅H₄, J(RhC) 4 Hz), 104.3 (C₈), 103.2 (C₉), 102.0 (C₁), 85.8 (C₅H₄, J(RhC) 3.8 Hz), 85.5 (C₅H₄, J(RhC) 3.8 Hz), 85.2 (C₅H₄, J(RhC) 3.6 Hz), 84.8 (C₅H₄, J(RhC) 3.7 Hz), 89.5 (C₂), 69.1 (C₃), 36.3 (C₁₀), 33.3 (C_{Me}), 32.0 (C_{Me}), 63.2 (2 C, J(RhC) 13.5 Hz, C_{Rhcod}), 63.1 (2 C, J(RhC) 13.5 Hz, C_{Rhcod}), 32.7 (4 C, C_{Rhcod}). **MS** (160 °C, EI) m/z = 570 (M⁺, 50 %), 486 (M–3 CO, 70 %), 406 (M–cod–2 CO, 30 %), 378 (M–cod–3 CO, 10 %), 323 (M–cod–Mn(CO)₃, 100 %).

Synthesis of [Rh(cod)(η⁵-C₅H₄)CMe₂(η⁵-C₉H₆)FeCp] (2d): 110 mg (0.25 mmol) of **2** were deprotonated by 0.2 ml BuLi in 20 ml THF. The blue solution prepared from 180 mg (0.42 mmol) [CpFe(fluorene)]PF₆ and 0.3 ml BuLi was added at 0 °C after 1 h. The reaction mixture was refluxed for 16 h and the solvent was removed. The residue was extracted by pentane / diethyl ether (1:1). The oily product **2d** was eluted from the chromatographic column with pentane / diethyl ether as a dark red band after fluorene and ferrocene in the first two fractions, respectively. Yield: 132 mg (0.24 mmol, 95 %). M(C₃₀H₃₃FeRh) = 552.33 g/mol; C: 65.48 (calc. 65.24); H: 6.21 (6.02) %.

NMR (C₆D₆) δ_H = 4.92 (2 H, m, C₅H₄), 4.85 (1 H, m, C₅H₄), 4.70 (1 H, m, C₅H₄), 4.67 (1 H, dd, J(HH) 2.7 + 0.7 Hz, H₂), 3.82 (1 H, d, J(HH) 2.7 Hz, H₃), 2.00 (6 H, br s, H_{Me}), 7.72 (1 H, m, H₇), 7.39 (1 H, m, H₄), 6.82 (1 H, m, H₆), 6.77 (1 H, H₅), 3.94 (4 H, m, H_{Rhcod}), 2.27 (4 H, m, H_{cod}), 1.98 (4 H, m, H_{cod}), 3.71 (5H, s, C_{Cp}). δ_C = 130.4, 129.8, 123.1, 123.0, 120.5 (C₅H₄, J(RhC) 4 Hz), 94.3 (C₈), 88.6 (C₉), 85.4 (C₁), 85.8 (2 C₅H₄, J(RhC) 3.8 Hz), 85.0 (C₅H₄, J(RhC) 3.7 Hz), 84.7 (C₅H₄, J(RhC) 3.7 Hz), 70.7 (C₂), 60.3 (C₃), 36.7 (C₁₀), 32.4 (2 C_{Me}), 63.0 (4C, J(RhC) 14 Hz, C_{Rhcod}), 32.9 (4 C, C_{Rhcod}), 69.3 (5 C_{Cp}). **MS** (140 °C, EI) m/z = 552 (M⁺, 90 %), 444 (M–cod, 100 %), 378 (M–cod–CpH, 20 %), 323 (M–cod–FeCp, 50 %).

Synthesis of [Ir(cod)(η⁵-C₅H₄)CMe₂(η⁵-C₉H₆)Rh(cod)] (3a): 0.14 ml butyllithium (1.5 mol/l) were added to a solution of 111 mg (0.21 mmol) of **3** in 20 ml THF and stirred at room temperature. After 2 h stirring, 52 mg (0.11 mmol) [Rh(cod)Cl]₂ were added to the red reaction mixture and stirred for another 2 hours. After removing the solvent, the reaction mixture was chromatographed on Al₂O₃. With pure hexane 145 mg (0.20 mmol, 94 %) of **3a** were obtained as a pale yellow solid. M(C₃₃H₄₀RhIr) = 731.79 g/mol; C: 53.98 (calc. 54.16); H: 5.72 (5.51) %.

NMR (C₆D₆) δ_H = 4.82 (2 H, t, J(HH) 2 Hz, C₅H₄), 4.63 (1 H, m, C₅H₄), 4.57 (1 H, m, C₅H₄), 5.90 (1 H, dd, J(HH) 2.8 + 2 Hz, H₂), 4.72 (1 H, dd, J(HH) 2.8 + 0.6 Hz, H₃), 1.76 (3 H, s, H_{Me}), 1.64 (3 H, s, H_{Me}), 7.50 (1 H, m, H₇), 7.16 – 7.0 (3 H, m, H_{4–6}), 4.07 (2 H, br m, H_{Rhcod}), 4.02 (2 H, br m, H_{Irircod}), 3.83 (4 H, br m, H_{cod}), 2.20 (4 H, m, H_{cod}), 1.98 – 1.65 (12 H, m, H_{cod}). δ_C = 122.7, 122.4, 120.6, 120.4, 114.1 (C₅H₄), 109.6 (C₈), 108.8 (C₉), 106.5 (C₁, J(RhC) 4 Hz), 93.1 (C₂, J(RhC) 5 Hz), 73.1 (C₃, J(RhC) 5 Hz), 82.1 (C₅H₄), 81.9 (C₅H₄), 80.2 (C₅H₄), 80.1 (C₅H₄), 36.6 (C₁₀), 31.2 (C_{Me}), 29.8 (C_{Me}), 68.5 (2 C, J(RhC) 13.6 Hz, C_{Rhcod}), 68.2 (2 C, J(RhC) 13.4 Hz, C_{Rhcod}), 32.1 (2 C, C_{Rhcod}), 31.3 (2 C, C_{Rhcod}), 46.5 (4 C_{Irircod}), 34.5 (2 C_{Irircod}), 34.4 (2 C_{Irircod}). **MS** (150 °C, EI) m/z = 732 (M⁺, 4 %), 622 (M–cod–H₂, 100 %), 407 (M–(Ind)Rh(cod), 20 %).

Synthesis of [Ir(cod)(η⁵-C₅H₄)CMe₂(η⁵-C₉H₆)Ir(cod)] (3b): 1.3 ml butyllithium (1.6 mol/l) were dropped to a THF solution of 220 mg (0.99 mmol) (C₅H₅)CMe₂(C₉H₇) in 20 ml diethyl ether and stirred for 4 h at room temperature. 672 mg (1 mmol) [Ir(cod)Cl]₂ were added and the orange reaction mixture was stirred for another 6 hours. After the solvent was removed *in vacuo*, the reaction mixture was filtered through a short column of Al₂O₃. 509 mg (0.62 mmol, 62 %) of [Ir(cod)(η⁵-Cp)CMe₂(η⁵-C₉H₆)Ir(cod)] **3b** could be isolated as a white solid with hexane. M(C₃₃H₄₀Ir₂) = 821.10 g/mol; C: 48.36 (calc. 48.27); H: 4.98 (4.91) %.

NMR (C₆D₆) δ_H = 4.81 (2 H, t, J(HH) 2 Hz, C₅H₄), 4.60 (1 H, t, J(HH) 2 Hz, C₅H₄), 4.52 (1 H, t, J(HH) 2 Hz, C₅H₄), 5.76 (1 H, d, J(HH) 2.7 Hz, H₂), 4.71 (1 H, dd, J(HH) 2.7 + 0.6 Hz, H₃), 1.67 (3 H, s, H_{Me}), 1.74 (3 H, s, H_{Me}), 7.48 (1 H, m, H₇), 7.1 – 6.9 (3 H, m, H_{4–6}), 3.96 (4 H, br m, H_{cod}), 3.82 (4 H, br m, H_{cod}), 2.23 (4 H, m, H_{cod}), 1.95 (4 H, m, H_{cod}), 1.9 – 1.6 (8 H, m, H_{cod}). δ_C = 123.6, 123.3, 121.8, 121.7, 114.1 (C₅H₄), 109.6 (C₈), 108.8 (C₉), 100.6 (C₁), 84.8 (C₂), 82.13 (C₅H₄), 82.08 (C₅H₄), 80.1 (C₅H₄), 80.0 (C₅H₄), 69.6 (C₃), 36.3 (C₁₀), 31.2 (C_{Me}), 29.2 (C_{Me}), 46.5 (4 C, C_{cod}), 34.5 (2 C, C_{cod}), 34.3 (2 C, C_{cod}), 51.2 (2 C, C_{cod}), 51.0 (2 C, C_{cod}), 33.6 (2 C, C_{cod}), 32.9 (2 C, C_{cod}). **MS** (150 °C, EI) m/z = 820 (M⁺, 100 %), 710 (M–cod–H₂, 70 %), 413 (M–Ir(cod)₂, 75 %), 407 (M–(Ind)Ir(cod), 45 %).

Synthesis of [Ir(cod)(η⁵-C₅H₄)CMe₂(η⁵-C₉H₆)Mn(CO)₃] (3c): 0.22 ml butyllithium (1.6 mol/l) were given to a solution of 180 mg (0.34 mmol) of **3** in 20 ml THF and stirred at room temperature. After 2 h stirring, 100 mg (0.36 mmol) [Mn(CO)₅Br] were added.

The orange solution was stirred for another hour followed by refluxing for another 6 h. After changing the solvent to pentane / diethyl ether the reaction mixture was first filtered through Al_2O_3 to remove the by-product $[\text{Mn}_2(\text{CO})_{10}]$ as the bright yellow band. After chromatography of the second fraction on a longer column of Al_2O_3 , 121 mg (0.18 mmol, 54 %) of **3c** were isolated as a yellow solid with a hexane / diethyl ether mixture (10 % diethyl ether). $\text{M}(\text{C}_{28}\text{H}_{28}\text{IrMnO}_3) = 659.68 \text{ g/mol}$; C: 50.74 (calc. 50.98); H: 4.55 (4.28) %.

NMR (C_6D_6) $\delta_{\text{H}} = 4.90$ (2 H, t, $J(\text{HH})$ 2 Hz, C_5H_4), 4.57 (2 H, t, $J(\text{HH})$ 2 Hz, C_5H_4), 4.42 (1 H, d, $J(\text{HH})$ 2.4 Hz, H_2), 4.46 (1 H, d, $J(\text{HH})$ 2.4 Hz, H_3), 1.75 (3 H, s, H_{Me}), 1.69 (3 H, s, H_{Me}), 7.42 (1 H, d, $J(\text{HH})$ 8 Hz, H_7), 7.0 – 7.16 (3 H, m, H_{4-6}), 3.80 (4 H, br s, H_{cod}), 2.20 (4 H, m, H_{cod}), 1.94 (4 H, m, H_{cod}). $\delta_{\text{C}} = 126.6, 126.5, 125.5, 124.9, 112.0$ (C_5H_4), 104.4 (C_8), 104.0 (C_9), 102.0 (C_1), 82.9 (C_5H_4), 82.7 (C_5H_4), 80.6 (C_5H_4), 80.0 (C_5H_4), 89.7 (C_2), 69.2 (C_3), 35.5 (C_{10}), 32.5 (C_{Me}), 31.8 (C_{Me}), 46.6 (4 C_{cod}), 34.3 (4 C_{cod}). **MS** (160 °C, EI) $m/z = 660$ (M^+ , 55 %), 576 ($\text{M}-3 \text{ CO}$; 100 %), 496 ($\text{M}-\text{cod}-2 \text{ CO}$, 4 %), 413 ($\text{M}-\text{cod}-\text{Mn}(\text{CO})_3$, 30 %), 363 ($\text{CpIr}(\text{cod})-3 \text{ H}$, 10 %).

Synthesis of $[\text{Ir}(\text{cod})(\eta^5\text{-C}_5\text{H}_4)\text{CMe}_2(\eta^5\text{-C}_9\text{H}_6)\text{FeCp}]$ (3d**):** 230 mg (0.44 mmol) of **3** were deprotonated by 0.3 ml BuLi in 20 ml THF. The blue solution prepared from 200 mg (0.46 mmol) $[\text{CpFe}(\text{fluorene})]\text{PF}_6$ and 0.3 ml BuLi was added at 0 °C after 1 h. The reaction mixture was refluxed for 16 h before the solvent was removed. The solid was extracted with pentane / diethyl ether (1:1). Fluorene and ferrocene were removed by sublimation at 50 °C before the residue was filtered over Al_2O_3 with pentane. After some educt **3**, the oily product **3d** (145 mg, 0.23 mmol, 51 %) was eluted secondly as a dark red band with pentane / diethyl ether. $\text{M}(\text{C}_{30}\text{H}_{33}\text{FeIr}) = 641.65 \text{ g/mol}$; C: 55.97 (calc. 56.16); H: 4.98 (5.18) %.

NMR (C_6D_6) $\delta_{\text{H}} = 4.85$ (2 H, t, $J(\text{HH})$ 2 Hz, C_5H_4), 4.61 (2 H, t, $J(\text{HH})$ 2 Hz, C_5H_4), 4.67 (1 H, dd, $J(\text{HH})$ 2.6 + 0.6 Hz, H_2), 3.79 (1 H, d, $J(\text{HH})$ 2.6 Hz, H_3), 1.94 (3 H, s, H_{Me}), 1.93 (3 H, s, H_{Me}), 7.70 (1 H, m, H_7), 7.35 (1 H, m, H_4), 6.81 (1 H, m, H_6), 6.77 (1 H, H_5), 3.81 (4 H, m, H_{cod}), 2.20 (4 H, m, H_{cod}), 1.98 (4 H, m, H_{cod}), 3.67 (5 H, s, C_{Cp}). $\delta_{\text{C}} = 130.4, 129.8, 123.2, 123.0, 114.0$ (C_5H_4), 93.3 (C_8), 88.6 (C_9), 85.3 (C_1), 81.9 (C_5H_4), 81.8 (C_5H_4), 80.5 (C_5H_4), 80.1 (C_5H_4), 70.8 (C_2), 60.3 (C_3), 35.5 (C_{10}), 32.2 (C_{Me}), 32.0 (C_{Me}), 46.5 (2 C_{cod}), 46.4 (2 C_{cod}), 34.5 (2 C_{cod}), 34.4 (2 C_{cod}), 69.3 (5 C_{Cp}). **MS** (140 °C, EI) $m/z = 642$ (M^+ , 100 %), 627 ($\text{M}-\text{Me}$, 15 %), 532 ($\text{M}-\text{cod}-\text{H}_2$, 25 %), 413 ($\text{M}-\text{cod}-\text{FeCp}$, 20 %).

Synthesis of $[\text{Mn}(\text{CO})_3(\eta^5\text{-C}_5\text{H}_4)\text{CMe}_2(\eta^5\text{-C}_9\text{H}_6)\text{Rh}(\text{cod})]$ (4a**):** When 0.14 ml butyllithium (1.5 mol/l) were added to a solution of 55 mg (0.15 mmol) of **4** in 20 ml THF, the solution color changed immediately from yellow to red. After 2 h stirring 40 mg (0.08 mmol) $[\text{Rh}(\text{cod})\text{Cl}]_2$ were added to the red reaction mixture and stirred for another 4 hours. After removing the solvent, the residue was chromatographed on Al_2O_3 . With hexane / diethyl ether 65 mg (0.11 mmol, 73 %) of **4a** were obtained as a yellow solid. $\text{M}(\text{C}_{28}\text{H}_{28}\text{RhMnO}_3) = 570.36 \text{ g/mol}$; C: 59.33 (calc. 58.96); H: 5.11 (4.95) %.

NMR (C_6D_6) $\delta_{\text{H}} = 4.39$ (1 H, td, $J(\text{HH})$ 2.8 + 1.7 Hz, C_5H_4), 4.27 (1 H, td, $J(\text{HH})$ 2.8 + 1.7 Hz, C_5H_4), 3.74 (1 H, td, $J(\text{HH})$ 2.8 + 1.7 Hz, C_5H_4), 3.65 (1 H, td, $J(\text{HH})$ 2.8 + 1.7 Hz, C_5H_4), 5.73 (1 H, dd, $J(\text{HH})$ 2.9 + 2 Hz, H_2), 4.48 (1 H, dd, $J(\text{HH})$ 2.9 + 0.6 Hz, H_3), 1.53 (3 H, s, H_{Me}), 1.39 (3 H, s, H_{Me}), 7.28 (1 H, m, H_7), 7.05 (3 H, m, H_{4-6}), 3.93 (4 H, m, H_{Rhcod}), 1.18 (4 H, m, H_{cod}), 1.35 (4 H, m, H_{cod}). $\delta_{\text{C}} = 225.9$ (3 C_{CO}), 123.0, 122.5, 120.8, 119.7, 113.7 (C_5H_4), 113.7 (C_8 , $J(\text{RhC})$ 2.6 Hz), 112.3 (C_9 , $J(\text{RhC})$ 1.8 Hz), 105.4 (C_1 , $J(\text{RhC})$ 4 Hz), 92.7 (C_2 , $J(\text{RhC})$ 5 Hz), 73.4 (C_3 , $J(\text{RhC})$ 5 Hz), 84.9 (C_5H_4), 84.3 (C_5H_4), 79.5 (C_5H_4), 79.2 (C_5H_4), 35.9 (C_{10}), 30.8 (C_{Me}), 28.5 (C_{Me}), 68.5 (2 C, $J(\text{RhC})$ 13.2 Hz, C_{cod}), 68.8 (2 C, $J(\text{RhC})$ 13.5 Hz, C_{cod}), 32.0 (2 C, C_{cod}), 31.1 (2 C, C_{cod}). **MS** (150 °C, EI) $m/z = 570$ (M^+ , 50 %), 486 ($\text{M}-3\text{CO}$, 30 %), 434 ($\text{M}-\text{cod}-\text{CO}$, 40 %), 406 ($\text{M}-\text{cod}-2 \text{ CO}$, 100 %), 378 ($\text{M}-\text{cod}-3 \text{ CO}$, 30), 323 ($\text{M}-\text{cod}-\text{Mn}(\text{CO})_3$, 90 %).

Synthesis of $[\text{Mn}(\text{CO})_3(\eta^5\text{-C}_5\text{H}_4)\text{CMe}_2(\eta^5\text{-C}_9\text{H}_6)\text{Ir}(\text{cod})]$ (4b**):** Reaction was carried out in analogy to **4a**. **4b** was obtained as a

yellow solid in 75 % yield. $\text{M}(\text{C}_{28}\text{H}_{28}\text{IrMnO}_3) = 659.68 \text{ g/mol}$; C: 50.82 (calc. 50.98); H: 4.35 (4.28) %.

NMR (C_6D_6) $\delta_{\text{H}} = 4.34$ (1 H, td, $J(\text{HH})$ 2.8 + 1.7 Hz, C_5H_4), 4.23 (1 H, td, $J(\text{HH})$ 2.8 + 1.7 Hz, C_5H_4), 3.74 (1 H, td, $J(\text{HH})$ 2.8 + 1.7 Hz, C_5H_4), 3.65 (1 H, td, $J(\text{HH})$ 2.8 + 1.7 Hz, C_5H_4), 5.57 (1 H, d, $J(\text{HH})$ 2.6 Hz, H_2), 4.68 (1 H, dd, $J(\text{HH})$ 2.6 + 0.6 Hz, H_3), 1.49 (3 H, s, H_{Me}), 1.42 (3 H, s, H_{Me}), 7.28 (1 H, m, H_7), 7.05 – 6.90 (3 H, m, H_{4-6}), 3.85 (4 H, m, H_{cod}), 1.77 (8 H, m, H_{cod}). $\delta_{\text{C}} = 225.9$ (3 C_{CO}), 123.5, 123.9, 122.0, 120.9, 115.7 (C_5H_4), 108.6 (C_8), 109.8 (C_9), 99.7 (C_1), 84.9 (C_2), 69.9 (C_3), 84.4 (C_5H_4), 84.3 (C_5H_4), 79.5 (C_5H_4), 79.2 (C_5H_4), 35.8 (C_{10}), 30.7 (C_{Me}), 28.6 (C_{Me}), 51.5 (4 C_{cod}), 33.6 (2 C, C_{cod}), 32.7 (2 C, C_{cod}). **MS** (150 °C, EI) $m/z = 660$ (M^+ , 85 %), 576 ($\text{M}-3 \text{ CO}$; 100 %), 524 ($\text{M}-\text{cod}-\text{CO}$, 10 %), 496 ($\text{M}-\text{cod}-2 \text{ CO}$, 25 %), 468 ($\text{M}-\text{cod}-3 \text{ CO}$, 15 %), 413 ($\text{M}-\text{cod}-\text{Mn}(\text{CO})_3$, 30 %).

Synthesis of $[\text{Mn}(\text{CO})_3(\eta^5\text{-C}_5\text{H}_4)\text{CMe}_2(\eta^5\text{-C}_9\text{H}_6)\text{FeCp}]$ (4d**):** Reaction was carried out in analogy to **3d**. 65 % yield of **4d** were obtained after chromatography as a yellow solid. $\text{M}(\text{C}_{25}\text{H}_{21}\text{FeMnO}_3) = 480.22 \text{ g/mol}$; C: 62.81 (calc. 62.54); H: 4.62 (4.41) %.

NMR (C_6D_6) $\delta_{\text{H}} = 7.55$ (1 H, m, H_7), 7.33 (1 H, m, H_4), 6.78 (1 H, m, H_6), 6.74 (1 H, H_5), 4.33 (1 H, td, $J(\text{HH})$ 2.8 + 1.7 Hz, C_5H_4), 4.18 (1 H, td, $J(\text{HH})$ 2.8 + 1.7 Hz, C_5H_4), 3.75 (1 H, td, $J(\text{HH})$ 2.8 + 1.7 Hz, C_5H_4), 3.67 (1 H, td, $J(\text{HH})$ 2.8 + 1.7 Hz, C_5H_4), 4.65 (1 H, dd, $J(\text{HH})$ 2.7 + 0.7 Hz, H_2), 3.66 (1 H, d, $J(\text{HH})$ 2.7 Hz, H_3), 1.84 (3 H, s, H_{Me}), 1.67 (3 H, s, H_{Me}), 3.60 (5 H, s, C_{Cp}). $\delta_{\text{C}} = 129.9, 129.7, 123.6, 123.2, 115.6$ (C_5H_4), 93.3 (C_8), 88.6 (C_9), 85.2 (C_1), 85.0 (C_5H_4), 84.3 (C_5H_4), 79.3 (C_5H_4), 79.4 (C_5H_4), 70.3 (C_2), 69.3 (5 C_{Cp}), 60.7 (C_3), 35.0 (C_{10}), 31.8 (C_{Me}), 31.4 (C_{Me}). **MS** (140 °C, EI) $m/z = 480$ (M^+ , 85 %), 396 ($\text{M}-3 \text{ CO}$, 100 %), 330 ($\text{M}-3 \text{ CO}-\text{CpH}$, 15 %), 276 ($\text{M}-\text{Cp}-\text{Mn}(\text{CO})_3$, 60 %).

Synthesis of $[\text{CpFe}(\eta^5\text{-C}_5\text{H}_4)\text{CMe}_2(\eta^5\text{-C}_9\text{H}_6)\text{Rh}(\text{cod})]$ (5a**):** 0.4 ml butyllithium (1.6 mol/l) were dropped to a solution of 171 mg (0.50 mmol) of **5** in 20 ml THF. After 2 h 123 mg (0.25 mmol) $[\text{Rh}(\text{cod})\text{Cl}]_2$ were added to the reaction mixture and stirred for another 6 hours. After removing the solvent, the reaction mixture was chromatographed on Al_2O_3 . The orange-yellow band containing 229 mg (0.41 mmol, 83 %) of **5a** was eluted with pentane after the yellow fraction of unreacted starting material. $\text{M}(\text{C}_{20}\text{H}_{23}\text{Rh}) = 366.30 \text{ g/mol}$; C: 65.31 (calc. 65.58); H: 6.47 % (6.33) %.

NMR (C_6D_6) $\delta_{\text{H}} = 4.02$ (2 H, m, C_5H_4), 3.90 (2 H, m, C_5H_4), 5.74 (1 H, dd, $J(\text{HH})$ 2.8 + 2 Hz, H_2), 4.46 (1 H, dd, $J(\text{HH})$ 2.8 + 0.6 Hz, H_3), 1.76 (3 H, s, H_{Me}), 1.65 (3 H, s, H_{Me}), 7.51 (1 H, d, $J(\text{HH})$ 8 Hz, H_7), 7.06 (3 H, m, H_{4-6}), 4.03 (4 H, br m, H_{Rhcod}), 1.90–1.60 (8 H, m, H_{cod}), 4.02 (5 H, s, C_{Cp}). $\delta_{\text{C}} = 68.7$ (5 C_{Cp}), 122.5, 122.2, 120.6, 120.3, 112.3 (C_8 , $J(\text{RhC})$ 1.9 Hz), 113.5 (C_9 , $J(\text{RhC})$ 1.8 Hz), 107.9 (C_1 , $J(\text{RhC})$ 4 Hz), 101.3 (C_5H_4), 93.1 (C_2 , $J(\text{RhC})$ 5 Hz), 72.9 (C_3 , $J(\text{RhC})$ 5 Hz), 67.9 (C_5H_4), 67.3 (C_5H_4), 66.8 (C_5H_4), 66.7 (C_5H_4), 36.1 (C_{10}), 29.7 (C_{Me}), 29.5 (C_{Me}), 68.3 (2 C, $J(\text{RhC})$ 13.8 Hz, C_{cod}), 68.1 (2 C, $J(\text{RhC})$ 13.8 Hz, C_{cod}), 32.0 (2 C, C_{cod}), 31.3 (2 C, C_{cod}). **MS** (150 °C, EI) $m/z = 552$ (M^+ , 50 %), 444 ($\text{M}-\text{cod}$, 100 %), 378 ($\text{M}-\text{cod}-\text{CpH}$, 20 %), 323 ($\text{M}-\text{cod}-\text{CpFe}$, 60 %).

Synthesis of $[\text{CpFe}(\eta^5\text{-C}_5\text{H}_4)\text{CMe}_2(\eta^5\text{-C}_9\text{H}_6)\text{Ir}(\text{cod})]$ (5b**):** Reaction was carried out in analogy to **5a**. A yellow solid (48 % yield) of **5b** was obtained. $\text{M}(\text{C}_{30}\text{H}_{33}\text{FeIr}) = 641.65 \text{ g/mol}$; C: 55.88 (calc. 56.16); H: 5.08 (5.18) %.

NMR (C_6D_6) $\delta_{\text{H}} = 4.02$ (5 H, s, C_{Cp}), 4.00 (4 H, m, C_5H_4), 5.60 (1 H, d, $J(\text{HH})$ 2.7 Hz, H_2), 4.66 (1 H, dd, $J(\text{HH})$ 2.7 + 0.7 Hz, H_3), 1.68 (3 H, s, H_{Me}), 1.75 (3 H, s, H_{Me}), 7.48 (1 H, m, H_7), 7.10 – 6.90 (3 H, m, H_{4-6}), 3.85–3.95 (4 H, m, H_{cod}), 1.90–1.85 (8 H, m, H_{cod}). $\delta_{\text{C}} = 68.7$ (5 C_{Cp}), 123.4, 123.2, 121.8, 121.7, 115.7 (C_5H_4), 108.6 (C_8), 109.8 (C_9), 101.9 (C_1), 101.3 (C_5H_4), 84.7 (C_2), 70.3 (C_3), 67.0 (C_5H_4), 67.3 (C_5H_4), 66.8 (C_5H_4), 66.5 (C_5H_4), 36.8 (C_{10}), 29.6 (C_{Me}), 29.5 (C_{Me}), 50.7 (2 C_{cod}), 50.9 (2 C_{cod}), 33.6 (2 C, C_{cod}), 32.8 (2 C, C_{cod}). **MS** (150 °C, EI) $m/z = 642$ (M^+ , 100 %), 534 ($\text{M}-\text{cod}$, 40 %), 413 ($\text{M}-\text{cod}-\text{CpFe}$, 30 %).

Synthesis of $[\text{CpFe}(\eta^5\text{-C}_5\text{H}_4)\text{CMe}_2(\eta^5\text{-C}_9\text{H}_6)\text{Mn}(\text{CO})_3]$ (5c**):** 0.3 ml butyllithium (1.6 mol/l) were given to a solution of 165 mg (0.48 mmol) of **5** in 20 ml THF and stirred at room temperature. After 2 h stirring, 132 mg (0.48 mmol) $[\text{Mn}(\text{CO})_5\text{Br}]$ were added. The orange solution was stirred for another hour followed by refluxing for another 10 h. After changing the solvent to pentane /

diethyl ether, the reaction mixture was first filtered through Al_2O_3 to remove the byproduct $[\text{Mn}_2(\text{CO})_{10}]$ as the bright yellow band. After chromatography of the second fraction on a long column of Al_2O_3 , 180 mg (0.37 mmol, 78 %) of **5c** were isolated as a yellow solid with a hexane / diethyl ether mixture (10 % diethyl ether). $\text{M}(\text{C}_{25}\text{H}_{21}\text{FeMnO}_3) = 480.22 \text{ g/mol}$; C: 62.61 (calc. 62.54); H: 4.52 (4.41) %.

NMR (C_6D_6) $\delta_{\text{H}} = 7.42$ (1 H, dd, $J(\text{HH})$ 8 + 0.7 Hz, H_7), 6.71 (1 H, dt, $J(\text{HH})$ 8 + 0.7 Hz, H_4), 6.71 (1 H, td, $J(\text{HH})$ 8 + 0.7 Hz, H_6), 6.57 (1 H, td, $J(\text{HH})$ 8 + 0.7 Hz, H_5), 4.06 (2 H, m, C_5H_4), 3.98 (2 H, m, C_5H_4), 4.31 (1 H, d, $J(\text{HH})$ 3 Hz, H_2), 4.35 (1 H, d, $J(\text{HH})$ 3 Hz, H_3), 1.81 (3 H, s, H_{Me}), 1.67 (3 H, s, H_{Me}), 3.99 (5 H, s, C_{Cp}). $\delta_{\text{C}} = 126.5$, 126.4, 125.4, 124.9, 99.6 (C_5H_4), 105.7 (C_8), 104.0 (C_9), 102.1 (C_1), 89.7 (C_2), 68.7 (C_3), 68.9 (5 C_{Cp}), 67.7 (C_5H_4), 67.6 (C_5H_4), 67.4 (C_5H_4), 66.7 (C_5H_4), 35.0 (C_{10}), 31.6 (C_{Me}), 30.9 (C_{Me}), 225.8 (3 C_{CO}). **MS** (130 °C, EI) $m/z = 480$ (M^+ , 20 %), 424 ($\text{M}-2$ CO, 20 %), 396 ($\text{M}-3$ CO, 90 %), 227 ($\text{M}-\text{IndMn}(\text{CO})_3$, 100 %).

Synthesis of $[\text{CpFe}(\eta^5\text{-C}_5\text{H}_4)\text{CMe}_2(\eta^5\text{-C}_9\text{H}_6)\text{FeCp}]$ (5d**):** 2.0 ml butyllithium (1.6 mol/l) were dropped to a solution of 330 mg (1.49 mmol) ($\text{C}_5\text{H}_5\text{CMe}_2(\text{C}_9\text{H}_7)$) in 20 ml diethyl ether and stirred at room temperature. After 4 h stirring, the blue THF solution prepared from 1.35 g (3.1 mmol) $[\text{CpFe}(\text{fluorene})]\text{PF}_6$ and 2.0 ml BuLi was added. The reaction mixture was refluxed for 16 h before the solution was concentrated to 1 ml. The reaction mixture was quenched with 10 ml pentane and filtered over 1 cm of Al_2O_3 . Fluorene and ferrocene were removed from the dried filtrate by sublimation at 50 °C. The residue was filtered again with pentane over 6 cm of Al_2O_3 , 478 mg (0.74 mmol, 50 %) of $[\text{CpFe}(\eta^5\text{-C}_5\text{H}_4)\text{CMe}_2(\eta^5\text{-C}_9\text{H}_6)\text{FeCp}]$ **5d** were isolated as a deep red solid. $\text{M}(\text{C}_{27}\text{H}_{26}\text{Fe}_2) = 642.19 \text{ g/mol}$; C 70.22 (calc. 70.16); H: 5.74 (5.67) %.

NMR (C_6D_6) $\delta_{\text{H}} = 7.72$ (1 H, m, H_7), 7.37 (1 H, m, H_4), 6.81 (1 H, dt, $J(\text{HH})$ 5 + 1.5 Hz, H_6), 6.78 (1 H, dt, $J(\text{HH})$ 5 + 1.5 Hz, H_5), 4.05 (2 H, m, C_5H_4), 3.93 (2 H, m, C_5H_4), 4.65 (1 H, dd, $J(\text{HH})$ 2.7 + 0.7 Hz, H_2), 3.67 (1 H, d, $J(\text{HH})$ 2.7 Hz, H_3), 2.02 (3 H, s, H_{Me}), 1.90 (3 H, s, H_{Me}), 3.70 (5 H, s, C_{Cp}), 4.05 (5 H, s, C_5H_4). $\delta_{\text{C}} = 130.4$, 129.8, 123.0, 122.9, 101.3 (C_5H_4), 94.4 (C_8), 88.6 (C_9), 85.1 (C_1), 67.1 (C_5H_4), 67.2 (C_5H_4), 67.1 (C_5H_4), 66.7 (C_5H_4), 70.8 (C_2), 69.2 (5 C_5H_4), 68.7 (5 C_{Cp}), 60.2 (C_3), 35.0 (C_{10}), 31.6 (C_{Me}), 31.1 (C_{Me}). **MS** (140 °C, EI) $m/z = 462$ (M^+ , 100 %), 447 ($\text{M}-\text{Me}$, 70 %), 276 ($\text{M}-\text{FeCp}_2$, 60 %), 261 ($\text{M}-\text{FeCp}_2-\text{Me}$, 20 %).

Synthesis of $[(\text{C}_9\text{H}_7)\text{CMe}_2(\eta^5\text{-C}_5\text{H}_4)\text{Fe}(\eta^5\text{-C}_5\text{H}_4)\text{CMe}_2(\eta^5\text{-C}_9\text{H}_6)\text{Ir}(\text{cod})]$ (6b**):** Reaction was carried out in analogy to **6a** [11]. 66 % yield of **6b** was obtained as a yellow solid. $\text{M}(\text{C}_{42}\text{H}_{45}\text{FeIr}) = 797.87 \text{ g/mol}$; C: 66.47 (calc. 66.22); H: 5.44 (5.68) %.

NMR: δ_{H} , (C_6D_6): 4.08 (8 H, m, C_5H_4), 5.82 (1 H, t, $J(\text{HH})$ 2.4 Hz, H_2), 5.64 (1 H, t, $J(\text{HH})$ 2 Hz, H_2), 4.67 (1 H, d, $J(\text{HH})$ 2.4 Hz, H_3), 2.96 (2 H, d, $J(\text{HH})$ 2 Hz, H_3), 1.76 (6 H, s, H_{Me}), 1.71 / 1.74 (each 3 H, s, H_{Me}), 7.60 (1 H, d, $J(\text{HH})$ 8 Hz, H_7), 7.50 (1 H, d, $J(\text{HH})$ 8 Hz, H_7), 7.20 (1 H, m, H_4), 7.16 – 7.0 (5 H, m, H_{4-6}), 3.98 (4 H, m, H_{cod}), 1.90 / 1.78 (each 4 H, m, H_{cod}). $\delta_{\text{C}} = 67.0$ – 68.5 (4 C_5H_4), 145.9 (C_8), 144.2 (C_9), 125.9, 124.3, 124.2, 123.4, 123.2, 122.7, 121.8, 121.7, 115.7 (C_5H_4), 102.0 (C_5H_4), 108.8 (C_8), 109.5 (C_9), 101.4 (C_5H_4), 101.1 (C_1), 84.7 (C_2), 69.4 (C_3), 66.9 – 69.4 (4 C_5H_4), 36.3 (C_{10}), 36.0 (C_{10}), 29.7 / 29.6 (C_{Me}), 28.6 (2 C_{Me}), 51.0 (2 C_{cod}), 50.9 (2 C_{cod}), 33.7 (2 C_{cod}), 32.9 (2 C_{cod}). **MS** (150 °C, EI) $m/z = 798$ (M^+ , 100 %), 688 ($\text{M}-\text{cod}-\text{H}_2$, 20 %), 573 ($\text{M}-\text{cod}-\text{H}_2-\text{Ind}$, 20 %), 413 ($(\text{Ind})\text{Ir}(\text{cod})-\text{H}_2$, 30 %), 267 ($\text{M}-\text{Ind}-(\text{Ind})\text{Ir}(\text{cod})$, 50 %).

Synthesis of $[(\text{C}_9\text{H}_7)\text{CMe}_2(\eta^5\text{-C}_5\text{H}_4)\text{Fe}(\eta^5\text{-C}_5\text{H}_4)\text{CMe}_2(\eta^5\text{-C}_9\text{H}_6)\text{Mn}(\text{CO})_3]$ (6c**):** Reaction was carried out in analogy to **5c** using 130 mg (0.26 mmol) of **6**, 0.2 ml butyllithium (1.6 mol/l) and 80 mg (0.29 mmol) $[\text{Mn}(\text{CO})_5\text{Br}]$. 70 mg (0.11 mmol, 42 %) of **6c** could be isolated by chromatography in the second fraction as a yellow solid with a hexane / diethyl ether mixture (10 % diethyl ether). $\text{M}(\text{C}_{37}\text{H}_{33}\text{FeMnO}_3) = 636.44 \text{ g/mol}$; C: 69.71 (calc. 69.83); H: 5.14 (5.23) %.

NMR (C_6D_6) $\delta_{\text{H}} = 7.60$ (1 H, d, $J(\text{HH})$ 8 Hz, H_7), 7.42 (1 H, d, $J(\text{HH})$ 8 Hz, H_7), 7.24 (1 H, m, H_4), 6.68 (1 H, t, $J(\text{HH})$ 8 + 1 Hz, H_5), 6.62 (1 H, td, $J(\text{HH})$ 8 + 1 Hz, H_6), 7.0 – 7.16 (3 H, m, $\text{H}_{4,5-6}$), 4.34 (2 H, m, C_5H_4), 4.04 (4 H, m, C_5H_4), 3.97 (2 H, m, C_5H_4), 3.88 (1 H, t, $J(\text{HH})$ 1.7 Hz, H_2),

4.11 (1 H, m, H_3), 5.82 (1 H, t, $J(\text{HH})$ 2 Hz, H_2), 2.96 (2 H, d, $J(\text{HH})$ 2 Hz, H_3), 1.80 / 1.68 (each 3 H, s, H_{Me}), 1.70 (6 H, s, H_{Me}). $\delta_{\text{C}} = 225.8$ (3 C_{CO}), 153.9 (C_1), 145.9 (C_8), 144.1 (C_9), 126.5, 126.4, 125.9, 125.4, 124.9, 124.4, 124.3, 122.7, 105.7 (C_8), 104.0 (C_9), 102.1 (C_1), 100.4 (C_5H_4), 99.6 (C_5H_4), 89.7 (C_2), 68.9 (C_3), 67.1 – 70.0 (8 C_5H_4), 37.1 (C_3), 36.3 (C_{10}), 35.2 (C_{10}), 28.7 / 28.6 (2 C_{Me}), 31.6 / 31.0 (2 C_{Me}). **MS** (130 °C, EI) $m/z = 636$ (M^+ , 100 %), 552 ($\text{M}-3$ CO, 20 %), 521 ($\text{M}-\text{Ind}$, 20 %), 396 ($\text{M}-3$ CO– IndCMe_2 , 100 %), 276 ($\text{M}-\text{Ind}-\text{IndMn}(\text{CO})_3$, 80 %).

Synthesis of $\{\text{Fe}[(\eta^5\text{-C}_5\text{H}_4)\text{CMe}_2(\eta^5\text{-C}_9\text{H}_6)\text{Ir}(\text{cod})]_2\}$ (7b**):** Reaction was carried out in analogy to **7a** [11]. The yellow solid of **7b** was obtained in 61 % yield. $\text{M}(\text{C}_{50}\text{H}_{56}\text{FeIr}_2) = 1097.26 \text{ g/mol}$; C: 54.97 (calc. 54.73); H: 5.32 (5.14) %.

NMR (C_6D_6) $\delta_{\text{H}} = 7.50$ (2 H, d, $J(\text{HH})$ 8 Hz, H_7), 7.0 – 7.16 (6 H, m, H_{4-6}), 4.05–3.88 (16 H, m, C_5H_4), 5.68 (1 H, t, $J(\text{HH})$ 2.4 Hz, H_2), 4.64 (1 H, d, $J(\text{HH})$ 2.4 Hz, H_3), 1.72 / 1.71 / 1.62 / 1.39 (each 3 H, s, H_{Me}), 1.90 / 1.78 (each 8 H, m, H_{cod}). $\delta_{\text{C}} = 123.4$, 123.2, 121.8, 121.7, 101.5 (2 C_5H_4), 109.5 (2 C_8), 108.5 (2 C_9), 102.0 (2 C_1), 84.7 (2 C_2), 69.4 (2 C_3), 67.8–68.2 (8 C_5H_4), 36.0 (2 C_{10}), 29.8 / 29.8 / 29.7 / 29.6 (4 C_{Me}), 50.9 (4 C_{cod}), 51.0 (4 C_{cod}), 33.7 (4 C_{cod}), 32.9 (4 C_{cod}). **MS** (170 °C, EI) $m/z = 1096$ (M^+ , 100 %), 986 ($\text{M}-\text{cod}-\text{H}_2$, 20 %), 878 ($\text{M}-2$ cod– H_2), 682 ($\text{M}-(\text{Ind})\text{Ir}(\text{cod})$, 10 %), 413 (30 %), 267 (50 %).

Synthesis of $\{\text{Fe}[(\eta^5\text{-C}_5\text{H}_4)\text{CMe}_2(\eta^5\text{-C}_9\text{H}_6)\text{Mn}(\text{CO})_3]_2\}$ (7c**):** Reaction was carried out in analogy to **6c** with the double stoichiometric amount of base and manganese reagent. **7c** could not be isolated from by-products by chromatography. **MS** (170 °C, EI) $m/z = 774$ (M^+ , 20 %), 718 ($\text{M}-2$ CO, 30 %).

Supporting material: Full Crystallographic data, ORTEP diagram for the structural analysis of the compounds **3a**, **3b** and **5c** and the CV of all species are available.

Acknowledgement. We like to thank the Deutsche Forschungsgemeinschaft (DFG) and the Graduiertenkolleg “Synthetische, mechanistische und reaktionstechnische Aspekte von Metallkatalysatoren” for financial support.

References

- [1] E. L. Muetterties, M. J. Krause, *Angew. Chem.* **1983**, 95, 135; *Angew. Chem. Int. Ed. Engl.* **1983**, 22, 135–148; D. A. Roberts, G. L. Geoffroy, in: G. Wilkinson, F. G. A. Stone, E. W. Abel (Eds.) *Comprehensive Organometallic Chemistry*, Vol. 6, Pergamon, Oxford, UK, 1982, Ch. 40, pp. 763–877; W. L. Gladfelter, G. L. Geoffroy, *Adv. Organomet. Chem.* **1980**, 18, 207; W. Beck, B. Niemer, M. Wieser, *Angew. Chem.* **1993**, 105, 969–996; *Angew. Chem. Int. Ed. Engl.* **1993**, 32, 923; S. Barlow, D. O'Hare, *Chem. Rev.* **1997**, 97, 637; E. L. Muetterties, R. N. Rhodin, E. Band, C. F. Brucker, W. R. Pretzer, *Chem. Rev.* **1979**, 79, 91; T. J. Marks, *Acc. Chem. Res.* **1992**, 25, 57; G. Süss-Fink, G. Meister, *Adv. Organomet. Chem.* **1993**, 35, 41; D. W. Stephan, *Coord. Chem. Rev.* **1989**, 95, 41; C. P. Casey, *J. Organomet. Chem.* **1990**, 400, 205; W. J. Sarain, J. P. Selegue, *Organometallics* **1989**, 8, 2153; M. D. Butts, R. G. Bergman, *Organometallics* **1994**, 13, 2668; B. Bosch, G. Erker, R. Fröhlich, *Inorg. Chim. Acta* **1998**, 270, 446; R. M. Bullock, C. P. Casey, *Acc. Chem. Res.* **1987**, 20, 167; E. Hey-Hawkins, *Chem. Rev.* **1994**, 95, 1661.
- [2] J. S. Drage, P. C. Vollhardt, *Organometallics* **1986**, 5, 280; T. E. Bitterwolf, *J. Organomet. Chem.* **1986**, 312, 197; W. Abriel, G. Baum, J. Heck, K.-A. Kriebisch, *Chem. Ber.* **1990**, 123, 1767.
- [3] J. A. Connor, *Top. Curr. Chem.* **1976**, 71, 71; P. V. Ivchenko, I. E. Nifante'ev, *Russ. J. Org. Chem.* **1998**, 34, 1.
- [4] H. Komatsu, H. Yamazaki, *J. Organomet. Chem.* **2001**, 634, 109; M. Fritz, J. Hiermeier, N. Hertkorn, F. H. Köhler, G. Müller, G. Reber, O. Steigemann, *Chem. Ber.* **1991**, 124, 1531;

- H. Atzkern, P. Bergerat, M. Fritz, J. Hiermeier, P. Hudeczek, O. Kahn, B. Kannellakopulos, F. H. Köhler, M. Ruhs, *Chem. Ber.* **1994**, 127, 277.
- [5] M. L. H. Green, N. Ishihara, *J. Chem. Soc., Dalton Trans.* **1994**, 657.
- [6] M. E. Rerek, L. N. Ji, F. Basolo, *J. Chem. Soc., Chem. Comm.* **1983**, 1208.
- [7] P. Escarpa, P. H. Moran, A.-N. Richartz, *J. Organomet. Chem.* **1998**, 559, 107; L. Djakovitch, W. A. Herrmann, *J. Organomet. Chem.* **1998**, 562, 71; M. L. H. Green, N. Ishihara, *J. Chem. Soc. Dalton Trans.* **1994**, 657; H. G. Alt, J. Su Han, U. Thewalt, *J. Organomet. Chem.* **1993**, 456, 89; H. G. Alt, J. Su Han, U. Thewalt, *J. Organomet. Chem.* **1993**, 445, 115; W. Spaleck, M. Antberg, V. Dolle, R. Klein, J. Rohrmann, A. Winter, *New J. Chem.* **1990**, 499; E. H. Licht, H. G. Alt, W. Milius, S. Abu-Orabi, *J. Organomet. Chem.* **1998**, 560, 69.
- [8] G. M. Diamond, A. N. Chernega, P. Mountford, M. L. H. Green, *J. Chem. Soc. Dalton Trans.* **1996**, 921; R. Fierro, T. E. Bitterwolf, A. L. Rheingold, G. P. A. Yap, L. M. Liable-Sands, *J. Organomet. Chem.* **1996**, 524, 19; R. Fierro, J. C. Chien, M. D. Rausch, *J. Polym. Sci.* **1994**, 32, 2817.
- [9] M. L. H. Green, N. H. Popham, *J. Chem. Soc., Dalton Trans.* **1999**, 1049; G. M. Diamond, M. L. H. Green, N. H. Popham, A. N. Chernega, *J. Chem. Soc., Chem. Commun.* **1994**, 727; P. Escarpa, *J. Organomet. Chem.* **2000**, 616, 29.
- [10] A. Decken, A. J. McKay, M. J. Brown, F. Bottomley, *Organometallics* **2002**, 21, 2006.
- [11] P. Escarpa, *J. Organomet. Chem.* **2000**, 616, 29.
- [12] S. Barlow, D. O'Hare, *Chem. Rev.* **1997**, 97, 637.
- [13] M. B. Robin, P. Day, *Adv. Inorg. Chem. Radiochem.* **1967**, 10, 247.
- [14] N. Camire, U. T. Müller-Westerhoff, W. E. Geiger, *J. Organomet. Chem.* **2001**, 637–639, 823.
- [15] a) H. Atzkern, P. Bergerat, M. Fritz, J. Hiermeier, P. Hudeczek, O. Kahn, B. Kannellakopulos, F. H. Köhler, M. Ruhs, *Chem. Ber.* **1994**, 127, 277. b) S. Rittinger, D. Buchholz, M.-H. Delville-Desbois, J. Linarès, F. Varret, R. Boese, L. Zsolnai, G. Huttner, D. Astruc, *Organometallics* **1992**, 11, 1454. c) P. Hudeczek, F. H. Köhler, *Organometallics* **1992**, 11, 1773. d) A. M. Gilbert, T. J. Katz, W. E. Geiger, M. P. Robben, A. L. Reingold, *J. Am. Chem. Soc.* **1993**, 115, 3199. e) W. E. Geiger, N. G. Connelly, *Adv. Organomet.* **1985**, 24, 87. f) P. Hudeczek, F. H. Köhler, P. Bergerat, O. Kahn, *Chem. Eur. J.* **1999**, 5, 70.
- [16] M.-H. Delville, *Inorg. Chim. Acta* **1999**, 291, 1.
- [17] a) S. P. Gubin, V. S. Khandkarova, *J. Organomet. Chem.* **1970**, 22, 449. b) C. Degrand, A. Radecki-Sudre, *J. Organomet. Chem.* **1984**, 268, 63. c) C. Degrand, J. Besancon, A. Radecki-Sudre, *J. Electroanal. Chem.* **1984**, 160, 199. d) C. Degrand, A. Radecki-Sudre, J. Besancon, *Organometallics* **1982**, 1, 1311. e) T. J. J. Müller, *J. Organomet. Chem.* **1999**, 578, 95. f) L. K. Young, J. E. Kim, Y. K. Chung, P. H. Rieger, D. A. Sweigart, *Organometallics* **1996**, 15, 3891.
- [18] S. Santi, A. Ceccon, L. Crociani, A. Gambaro, P. Ganis, M. Tiso, A. Venzo, A. Bacchi, *Organometallics* **2002**, 21, 565.
- [19] R. Cramer, *Inorg. Synth.* **1974**, 15, 14.
- [20] E. W. Abel, G. Wilkinson, *J. Chem. Soc.* **1959**, 1501.
- [21] H.-K. Lee, S.-G. Lee, S. S. Lee, Y. K. Chung, *Organometallics* **1997**, 16, 304.
- [22] Sheldrick, G. M. SHELXS-86, *Acta Crystallogr.* **1990**, A46, 467; Sheldrick, G. M. SHELXL-93, University of Göttingen, Germany **1993**.
- [23] R. Ahlrichs, M. Bär, M. Häser, H. Horn, C. Kölmel, *Chem. Phys. Lett.* **1989**, 162, 165.
- [24] A. D. Becke, *Phys. Rev. A* **1988**, 38, 3098.
- [25] J. P. Perdew, *Phys. Rev. B* **1986**, 33, 8822.
- [26] K. Eichkorn, O. Treutler, H. Öhm, M. Häser, R. Ahlrichs, *Chem. Phys. Lett.* **1995**, 242, 652.
- [27] a) A. Schäfer, C. Huber, R. Ahlrichs, *J. Chem. Phys.* **1994**, 100, 5829. b) K. Eichkorn, F. Weigend, O. Treutler, R. Ahlrichs, *Theor. Chem. Acc.* **1997**, 97, 331.
- [28] A. Schäfer, H. Horn, R. Ahlrichs, *J. Chem. Phys.* **1992**, 97, 2571.
- [29] D. Andrae, U. Häussermann, M. Dolg, H. Stoll, H. Preuss, *Theor. Chim. Acta* **1990**, 77, 123.